

MIGUEL LEITÃO RODRIGUES

WIRELESS INSTRUMENTED KNEE PAD FOR HUMAN GAIT ANALYSIS

Master's Dissertation in Electrical and Computer Engineering, supervised by Prof. António Paulo Mendes Breda Dias Coimbra, Prof. João Paulo Morais Ferreira, and Prof. Manuel Marques Crisóstomo and presented to the Faculty of Science and Technology of the University of Coimbra.

October 2021



UNIVERSIDADE D
COIMBRA



UNIVERSIDADE D
COIMBRA

MIGUEL LEITÃO RODRIGUES

**WIRELESS INSTRUMENTED KNEE PAD
FOR HUMAN GAIT ANALYSIS**

Dissertação no âmbito do Mestrado Integrado em Engenharia Eletrotécnica e de Computadores, especialização em Automação orientada pelo Professor António Paulo Mendes Breda Dias Coimbra, Professor João Paulo Morais Ferreira, e Professor Manuel Marques Crisóstomo e apresentada ao Departamento de Engenharia Eletrotécnica e de Computadores da Faculdade de Ciências e Tecnologia da Universidade de Coimbra.

Outubro 2021

“Ah, not in knowledge is happiness, but in the acquisition of knowledge.”

Edgar Allan Poe

Acknowledgements

Em primeiro lugar, quero expressar o meu sincero agradecimento aos meus orientadores Professor Doutor António Paulo Mendes Breda Dias Coimbra, Professor Doutor Manuel Marques Crisóstomo e Professor Doutor João Paulo Morais Ferreira pelo seu aconselhamento, orientação e suporte. Ajudaram-me não só a terminar esta etapa académica, mas também a expandir os meus conhecimentos e a melhorar a minha análise crítica.

Quero também agradecer a todas as pessoas que partilharam o meu percurso no DEEC e que fizeram parte do meu quotidiano enquanto estudante, em particular ao “Sr. Victor” porque mais do que uma boa companhia enquanto nos servia os seus famosos paniques e os seus cafés, foi também um professor e amigo, não no curso, mas na vida.

A todos os meus amigos que fiz no associativismo, seja no NEEEC, na Associação Académica ou na Secção de Fado, por terem contribuído para eu crescer como pessoa, tanto a nível pessoal como profissional.

Aos meus amigos de Coimbra de longa data, que por mais que cada um tenha seguido o seu curso e caminho, sempre me apoiaram e que quando reunidos nada muda.

Aos meus amigos e colegas DEECÓLICOS, por estarem sempre comigo nas melhores e piores alturas do meu percurso académico e pessoal. Sei que mais do que boas amizades, levo comigo uma segunda família.

À minha namorada, que foi um dos meus maiores suportes nesta etapa, pois sempre acreditou em mim, sempre me transmitiu a confiança necessária e me fez rir quando mais precisava.

Por último, mas não menos importante, quero agradecer à minha família. Aos meus avós, por desde cedo me ensinaram que é importante ser esforçado e trabalhar para atingirmos os nossos objetivos, mas sem nunca esquecer que o mais importante são as pessoas, em especial a família. Aos meus pais, que me permitiram ter os melhores anos da minha vida académica com toda a estabilidade e conforto que tive. Por terem depositado toda a sua confiança em mim e nas minhas capacidades, sem duvidar uma única vez, mesmo quando chegado a casa a altas horas da madrugada ou mesmo não chegando a casa por ter ficado a dormir em casa de alguém. E à minha irmã, que partilhou momentos comigo não só como irmão, como colega estudante, no associativismo e como “filhos únicos” quando um de nós se ausentava de casa sem regresso anunciado. Ao seu carismático apoio sempre com um sorriso e uma

palmadinha nas costas e com a sua emblemática frase “sim acredita, tu és mais forte e sabes que no fim vais vencer”!

A todos, o meu mais sincero obrigado.

Abstract

Human's walking is often affected by pathologies caused by neuromuscular and musculoskeletal injuries. The gait reconstruction of patients whose movement has been harmed due to these types of injuries varies depending on the intensity of the injury and on the patient's current recovery stage. As a result, it is advantageous to use a device that allows the collection of human gait data to determine the severity of the injury and quantify the degree of recovery in the rehabilitation phase.

This work developed and tested the feasibility of two Instrumented Knee Pad systems to analyse the Knee Sagittal Plane Angle to assist a doctor in detecting and quantifying human gait abnormalities. Compared to vision-based motion acquisition systems, these low-cost Instrumented Knee Pad systems are two separate versions with different data acquisition technologies, one with an absolute rotary encoder and the other with an IMU (Inertial Measuring Unit). Between the two methods, the version with the encoder turned out to have better results. The use of the Instrumented Knee Pad systems and the software application developed does not require any specific technical knowledge, making it an easy and practical tool for medical assistance in analysing the human gait.

Keywords: Human gait, Instrumented Knee Pad, Encoder, IMU, Wireless

Resumo

A marcha humana é frequentemente afetada por patologias causadas por lesões neuromusculares e músculo-esqueléticas. A reabilitação da marcha de pacientes cujo movimento foi prejudicado devido a estes tipos de lesão varia em função da intensidade da lesão e da fase de recuperação atual do paciente. Como resultado, é vantajoso utilizar um dispositivo que permita a recolha de dados relativos à marcha humana para determinar a gravidade da lesão e quantificar o grau de recuperação na fase de reabilitação.

Neste trabalho foi desenvolvido e testada a viabilidade de dois sistemas de Joelheiras Instrumentadas para a medição dos Ângulos do Plano Sagital dos Joelhos para assistir um médico a detetar e quantificar anomalias na marcha humana. Estes sistemas de Joelheiras Instrumentadas, de baixo custo comparativamente com os sistemas de aquisição de movimento com base em visão, são duas versões separadas com diferentes tecnologias de aquisição de dados, uma com um *encoder* rotativo absoluto e a outra com um IMU (*Inertial Measuring Unit*). Entre os dois métodos, a versão com o *encoder* acabou por ser a que apresentou melhores resultados. A utilização dos sistemas de Joelheiras Instrumentadas e a aplicação informática desenvolvida não necessitam de qualquer conhecimento técnico específico, tornando-se uma ferramenta fácil e prática para auxílio médico na análise da marcha humana.

Palavras-chave: Marcha humana, Joelheira Instrumentada, Encoder, IMU, Wireless

Contents

List of Figures.....	VII
List of Tables	IX
Acronyms	XI
1. Introduction	1
1.1. Motivation	1
1.2. Approach.....	1
1.3. Contributions	2
1.4. Thesis outline.....	2
2. Literature review	5
2.1. Human Gait	5
2.1.1. Gait Phases.....	5
2.1.2. The knee as an area of the Human body susceptible to injury.....	7
2.2. Clock Synchronisation Protocols.....	9
2.2.1. Network Time Protocol.....	9
2.2.2. Simple Network Time Protocol.....	11
2.2.3. Precision Time Protocol	11
2.3. Human Gait Analysis Related Works.....	14
2.3.1. Image Processing.....	14
2.3.1.1. Stereoscopic Vision.....	15
2.3.1.2. Time-of-Flight Systems (ToF).....	15
2.3.1.3. Laser Range Scanner.....	16
2.3.2. Wearable Sensors	17
2.3.2.1. Accelerometer, Gyroscope, and Magnetoresistive Sensors	17
2.3.2.2. Flexible Goniometer.....	18
2.3.2.3. Electromagnetic Tracking System (ETS).....	19
3. Developed System.....	21
3.1. Encoder Instrumented Knee Pad	21
3.1.1. Hardware Selection	21
3.1.2. System Assembly.....	22
3.1.2.1. System Structure.....	22
3.1.2.2. Connections Scheme	23
3.1.3. Software measuring system.....	24
3.2. IMU Instrumented knee pad	24

3.2.1.	Hardware Selection	24
3.2.2.	Connections Scheme	25
3.2.3.	Software measuring system.....	25
3.3.	Instrumented Knee Pads Synchronisation and Data Transferring.....	26
3.4.	Developed Application.....	28
3.5.	Instrumented Knee Pad Powering System.....	29
4.	Tests and Results	31
4.1.	Exam Procedure	31
4.2.	Data Processing.....	33
4.3.	Results and Discussion.....	34
5.	Conclusion and Future Work	47
5.1.	Conclusion.....	47
5.2.	Future Work.....	48
6.	References.....	49
APPENDIX A		53
APPENDIX B		59
APPENDIX C		63

List of Figures

FIGURE 1: GAIT PHASES IN A NORMAL GAIT CYCLE. (A) GAIT PHASES OF THE STANCE PERIOD; (B) GAIT PHASE OF THE SWING PERIOD (ADAPTED FIGURE [4])	6
FIGURE 2: ARTICULAR ANGLES OF THE LEFT KNEE IN THE SAGITTAL PLANE DURING A GAIT CYCLE IN THREE VOLUNTEERS [7].	8
FIGURE 3: LITERATURE REFERENCE CURVE FOR KNEE SAGITTAL PLANE ANGLE CURVE (ADAPTED FROM [8])	9
FIGURE 4: EXCHANGE OF MESSAGES IN THE NTP PROTOCOL [9].....	10
FIGURE 5: PTP OPERATION [9].....	12
FIGURE 6: DIFFERENT TECHNOLOGIES FOR IP BASED MEASUREMENT [14].	15
FIGURE 7: TIME-OF-FLIGHT WORKING PRINCIPLE [14].	16
FIGURE 8: THE MODEL OF MAGNETORESISTIVE EFFECT. (A) CURRENT MODE UNDER NON-MAGNETIC FIELD; (B) CURRENT MODE UNDER MAGNETIC FIELD [2].	18
FIGURE 9: CUI-AMT22 PACK: (1) CUI-AMT22 ENCODER, (2) HOLDING BACK CASES, (3) CENTRE FIXING PIECES, (4) MOUNTING TOOLS	22
FIGURE 10: (1) THIGH RPS, (2) CENTRAL AXEL, (3) CALF RPS	22
FIGURE 11: SCHEME CONNECTIONS BETWEEN ENCODER AND WEMOS D1 MINI BOARD.....	23
FIGURE 12: IMU INSTRUMENTED KNEE PAD - PLACEMENT	24
FIGURE 13: SCHEME CONNECTIONS BETWEEN IMU AND WEMOS D1 MINI BOARD	25
FIGURE 14: STABLISH NEW WI-FI CONNECTION THROUGH THE DEVELOPED APPLICATION	27
FIGURE 15: PATIENT OVERVIEW>REFERENCE SUBPAGE	29
FIGURE 16: PLACING ENCODER INSTRUMENTED KNEE PAD ON THE PATIENT LEG	31
FIGURE 17: ENCODER INSTRUMENTED KNEE PAD HOLDING STRAPS	31
FIGURE 18: AFTER SETTING UP THE ENCODER KNEE PADS: (A) STANDING, (B) WALKING.....	32
FIGURE 19: A) FRONT SIDE OF THE LEG, B) LATERAL SIDE OF THE LEG	32
FIGURE 20: (A) MARKS FOR ALIGNMENT ON THE FABRIC STRAPS, (B) PENDULUM ALIGN IMU INSTRUMENTED KNEE PAD	32
FIGURE 21: VERIFICATION OF THE ENCODER IKP COLLECTED VALUES VS MEASURED PROTRACTOR VALUES (1) FIRST STAND, (2) FIRST SIT, (3) SECOND STAND, (4) SECOND SIT, (5) THIRD STAND, (6) THIRD SIT.	35
FIGURE 22: SITTING AND STANDING UP IKP MOVEMENT CURVE.....	36
FIGURE 23: VERIFICATION OF THE IMU IKP COLLECTED VALUES VS MEASURED PROTRACTOR VALUE – (1) 0°, (2) 30°.	37
FIGURE 24: VERIFICATION OF THE IMU IKP COLLECTED VALUES VS MEASURED PROTRACTOR VALUES – (3) 60°, (4) 90°.	37

FIGURE 25: ENCODER AND IMU IKPS GAIT CURVES FROM 10 METERS WALKING TEST	38
FIGURE 26: ENCODER IKP BEST WALKING GAIT CURVE	39
FIGURE 27: IMU IKP BEST WALKING GAIT CURVE.....	40
FIGURE 28: ENCODER IKP GAIT CURVES FROM FIVE HEALTHY VOLUNTEERS	40
FIGURE 29: ENCODER IKP DIFFERENT VELOCITY GAIT CURVES FROM A HEALTHY WOMAN.....	41
FIGURE 30: ENCODER IKP GAIT CURVES FROM A HEALTHY WOMAN - DIFFERENT TIME DURATION TESTS	42
FIGURE 31: ENCODER IKP GAIT CURVES FOR THE TWO LEGS - HEALTHY MAN.....	43
FIGURE 32: ENCODER IKP GAIT CURVES FOR THE TWO LEGS - HURT MAN	44
FIGURE 33: KNEES SAGITTAL JOINT ANGLES TRAJECTORIES WHEN GOING UPSTAIRS.....	45
FIGURE 34: KNEES SAGITTAL JOINT ANGLES TRAJECTORIES WHEN GOING DOWNSTAIRS.....	45

List of Tables

TABLE 1: PIN CONNECTIONS BETWEEN ENCODER AND WEMOS D1 MINI BOARD	23
TABLE 2: PIN CONNECTIONS BETWEEN IMU AND WEMOS D1 MINI BOARD	25
TABLE 3: SITTING AND STANDING UP MOVEMENT READINGS – IKP AND PROTRACTOR	36
TABLE 4: GAIT PARAMETERS FROM FIVE HEALTHY MEN	41
TABLE 5: GAIT PARAMETERS FROM A HEALTHY WOMAN – THREE DIFFERENT VELOCITIES	42
TABLE 6: GAIT PARAMETERS FROM A HEALTHY WOMAN – THREE DIFFERENT TEST DURATION.....	43
TABLE 7: GAIT PARAMETERS FROM A HEALTHY MAN – LEFT AND RIGHT LEGS.....	44
TABLE 8: GAIT PARAMETERS FROM A HURT MAN – LEFT AND RIGHT LEGS	44

Acronyms

ETS	Electromagnetic Tracking System
IP	Image Processing
IMU	Inertial Measurement Unit
IKP	Instrumented Knee Pad
IP	Internet Protocol
KSPA	Knee Sagittal Plane Angle
KSPAC	Knee Sagittal Plane Angle Curve
NTP	Network Time Protocol
PTP	Precision Time Protocol
RPS	Rigid Plastic Structures
SNTP	Simple Network Time Protocol
UCT	Universal Coordinated Time
UDP	User Datagram Protocol
WFA	Windows Forms Application

1. Introduction

This thesis presents an approach to recognise and quantify alterations in the human's gait normality through instrumentation. The aim is to know the knees' angles in real-time and the synchronisation between the legs—the implementation of this concept results in a scalable, robust, computationally simple and easy-to-use Instrumented knee pad (IKP).

1.1. Motivation

Similar studies have inspired this system in human gait analysis. Previous studies have presented examples of systems to characterise human gait in different manners—some of these use instrumented shoes or instrumented soles.

Scientific literature defines the human gait as a flowing, continuous and cyclical movement. Multiple pathologies will quickly disrupt these human gait characteristics, resulting in physical dysfunction and a decline in an individual's quality of life. Identifying, analysing, fixing, and tracking these gait variations are essential steps in improving patients' quality of life. However, it is not easy to recognise alterations in the human gait's normality since each person has a different walk and physiognomy.

As a result, an Instrumented knee pad system was developed that helps to overcome the limitations of conventional diagnostic methods currently used. This system allows a more objective knowledge of the patient's evolution with gait disorders, enabling a more personalised and effective rehabilitation.

1.2. Approach

At the beginning of this work, the Knee Sagittal Plane Angle Curve (KSPAC) was the focused matter. For that, were developed two systems with two ways of measuring the KSPAC. The first system, placed at the back of the leg, uses a rotative encoder linked to a pivoting structure with a rotating shaft. The second method to measure the KSPAC uses two IMUs for each leg. Each IMU is held by a fabric strap, aligned and placed at the front of the thigh and shin.

The sensors are connected to a mini development board with Wi-Fi in both methods, which sends the collected data to a computer with a Windows Forms Application (WFA) developed to save and process the data.

After all hardware and software were concluded, some tests were conducted to confirm if the collected data from the two knee pad systems corresponds to the established literature values.

1.3. Contributions

In this dissertation, the Instrumented knee pad (IKP) approach proposes to overcome the limitations of conventional diagnostic methods currently used. This IKP can complement human gait study and characterisation, which may constitute a modern and essential low-cost medical tool. It may also allow a more objective knowledge of a patient's evolution with gait disorders, enabling a more personalised and effective rehabilitation by tracking improvements in a human gait recovery.

The IKP can also be used to monitor incorrect movements in the sports field, thus making IKPs a multi-purpose tool.

1.4. Thesis outline

The thesis proceeds as follows:

Chapter 2 examines the related literature on human gait science and sets the knee injuries as a rupture in human gait normality. Synchronisation protocols and previous works are also described.

Chapter 3 describes how the two Instrumented Knee Pads (IKPs) systems were made, the materials used, and the electric connections. It is also explained how the data is collected into the developed computer application and that application layout.

Chapter 4 establishes the procedures and conditions to run the tests with the IKPs, like setting the IKPs in the legs, the environment, footwear and space to travel/time count. Thereafter describes how the collected data was analysed and the validation findings of the IKPs systems.

Chapter 5 points out the conclusions taken from the developed work in this thesis. It also described some different functionalities and tests with the developed IKP systems as future works.

Appendix A includes the Instrumented Knee Pads assembling process with photographic register.

Appendix B presents the relevant code developed for the data collection in C++ and the Matlab code developed for the data analysis.

Appendix C includes visual information about the developed application, presenting the applications pages and their purpose.

2. Literature review

This chapter summarises the relevant literature on human gait research. It sets the knee as one of the most vulnerable areas for gait injury, followed by an analysis of the Knee Sagittal Plane Angle Curve (KSPAC).

Clock synchronisation protocols are presented in this thesis to justify the protocol used to set each Instrumented knee pad in the same timeline.

A brief review of other existent equipment and systems to analyse the KSPAC is also presented in this chapter.

2.1. Human Gait

Human gait has been an object of study for many years. From the gait study, it is possible to know the human biomechanics, diagnose patterns, supervise improvements after therapeutic intervention, correct pathological gait patterns and prevent additional pathologies [1].

Gait pathologies are divided into two groups: neuromuscular or musculoskeletal etiologies. Central nervous system cerebrovascular diseases and cerebellar degeneration are the most prominent of neuromuscular impact. The most prominent musculoskeletal causes are the difference in the length of the legs and the hip, knee, foot and ankle pathologies.

In order for an individual to walk correctly, the following conditions must be verified [1]:

- **Musculoskeletal integrity:** functioning of bones, joints and muscles;
- **Neurological control:** reception and integration of messages coming from the brain to locate the body in space;
- **Balance:** ability to maintain the vertical position;
- **Locomotion:** ability to initiate and maintain rhythmic gait.

2.1.1. Gait Phases

Generally, human gait is a periodic movement of the body segments and includes repetitive motions. To better understand this periodic gait course, the gait phase must describe an entire gait period. In the past, regular events were conventionally used as the critical actions of separated gait phases. However, this method only worked for amputees,

and it frequently failed to accommodate the gait abnormalities of individuals with paralysis or arthritis [2].

Analysis of the human gait pattern by phases more directly identifies the functional significance of the different motions generated at the individual joints and segments. A normal human gait cycle is divided into eight different gait phases: initial contact, loading response, midstance, terminal stance, pre-swing, initial swing, mid-swing, and terminal swing (Figure 1) [2] [3].

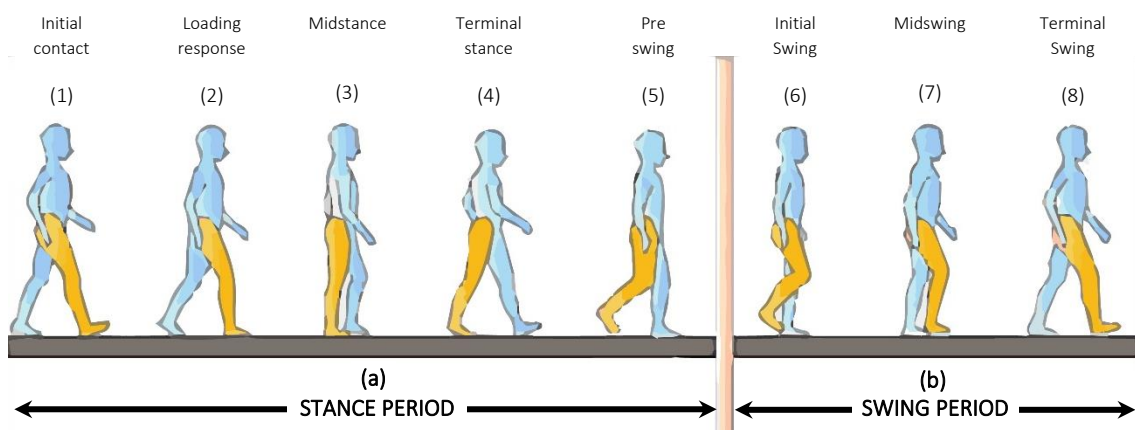


Figure 1: Gait phases in a normal gait cycle. (a) gait phases of the stance period; (b) gait phase of the swing period (adapted figure [4])

(1) Initial contact: This phase comprises the moment when the foot touches the floor. The joint postures presented at this time determine the limb's loading response pattern.

(2) Loading response: This phase is the initial double-stance period. The phase begins with initial floor contact and continues until the other foot is lifted for swing. While the heel rocks the body, the knee is flexed for shock absorption. Ankle plantarflexion limits the heel rocker through forefoot contact with the floor.

(3) Midstance: This phase is the first half of the single-limb support interval. In this phase, the limb advances over the stationary foot through ankle dorsiflexion (ankle rocker) while the knee and hip extend. Midstance begins when the other foot is lifted and continues until body weight is aligned over the forefoot.

(4) Terminal stance: This phase completes the single-limb support. The stance begins with the heel rising and continues until the other foot strikes the ground, in which the heel rises and the limb advances over the forefoot rocker. Throughout this phase, bodyweight moves ahead of the forefoot.

(5) Pre-swing: This final stance phase is the second double-stance interval in the gait cycle. Pre-swing begins with the initial contact of the opposite limb and ends with the ipsilateral toe-off. The objective of this phase is to position the limb for swing.

(6) Initial swing: This phase is approximately one-third of the swing period, beginning with a lift of the foot from the floor and ending when the swinging foot is opposite the stance foot. In this phase, the foot is lifted, and the limb is advanced by hip flexion and increased knee flexion.

(7) Mid-swing: This phase begins as the swinging limb is opposite the stance limb and ends when the swinging limb is forward, and the tibia is vertical (i.e., hip and knee flexion postures are equal). The knee is allowed to extend in response to gravity, while the ankle continues dorsiflexion to neutral.

(8) Terminal swing: This final swing phase begins with a vertical tibia and ends when the foot strikes the floor. Limb advancement is completed as the leg (shank) moves ahead of the thigh. In this phase, limb advancement is completed through knee extension. The hip maintains its earlier flexion, and the ankle remains dorsiflexed to neutral.

Each gait phase has a functional objective and a critical pattern of selective synergistic motion to accomplish its goal. The sequential combination of the phases also enables the limb to accomplish three basic tasks: weight acceptance, single-limb support, and limb advancement. Weight acceptance begins the stance period through initial contact and loading response. Single-limb support continues the stance through the midstance and terminal stance. Limb advancement begins in the pre-swing phase and continues through initial swing, mid-swing, and terminal swing.

Based on the above analysis of the gait phases and basic limb movement tasks, the gait phases may be detected effectively after orientations of the leg segments are accurately obtained [2] [5].

2.1.2. The knee as an area of the Human body susceptible to injury

The knee is one of the areas of the human body most susceptible to be injured because it is the central joint for the execution of human gait, as stated by José H. M. Fernandes [6]:

“The knee joint is particularly susceptible to traumatic injury because it is located at the ends of two long lever arms, the tibia and femur. Because the joint connects a long bone

“sitting” on top of another long bone, its strength and stability depend on the surrounding ligaments and muscles, not just its bony configuration.”

“Due to its anatomical arrangement, the knee is an area whose assessment is difficult, and the examiner must spend time to ensure that all structures are tested. Besides, it should be noted that the lower back, hip and ankle can produce pain and consequently disable mobility in the area of the knee.”

The various joints involved in human gait are shoulders, elbows, wrists, hips, knees, ankles, heels and toes. Only the knee joint movement will be studied in this work, specifically, the Knee Sagittal Plane Angle Curve (KSPAC), whose profile is represented in Figure 2, representing the KSPACs of three women with a normal gait analysed in [7]. These KSPACs present the values of the angles formed by the knee throughout a gait cycle.

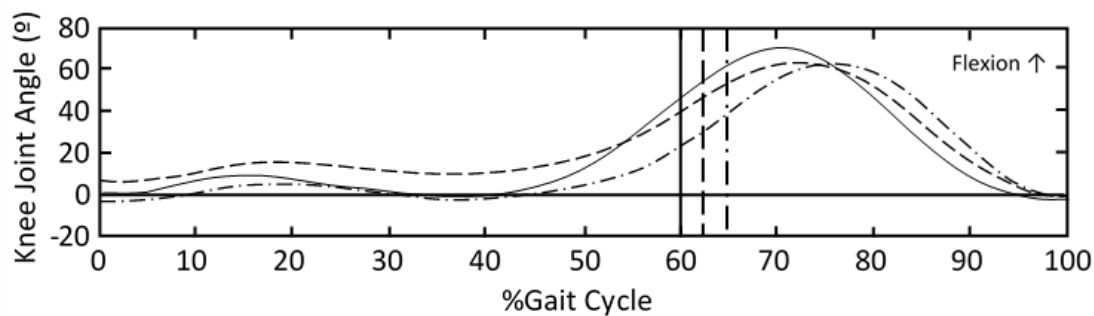


Figure 2: Articular angles of the left knee in the sagittal plane during a gait cycle in three volunteers [7].

Figure 2 shows that two flexions describe the knee motion. The KSPAC starts with a value close to zero, consisting of the initial contact, followed by the first flexion wave, which describes the first double support, responsible for absorbing shock, aiding weight transfer, and shortening the length of the lower limb. The first wave of flexion is followed by the single support in which knee extension occurs. The second double support begins the second wave of flexion, which reaches its maximum value at the beginning of the swing phase to assist the foot’s movement away from the ground. Finally, the amplitude of the KSPAC decreases until the limb begins a new initial contact [7].

Figure 3 depicts a KSPAC that describes the average movement that an ordinary individual is expected to perform, free of gait limitations and pathologies.

Physicians and physical therapists use a KSPAC like the literature reference curve (LRC) to analyse their patients. KSPACs with a slight deviation from the LRC do not indicate

any pathology. However, significant deviations already represent pathology, and the larger the deviation, the greater the severity of the pathology.

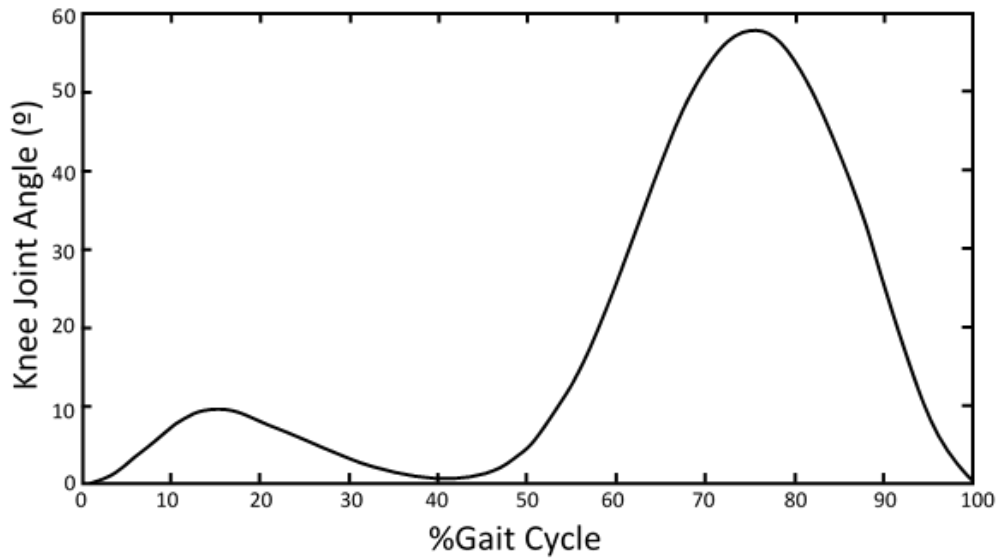


Figure 3: Literature reference curve for knee sagittal plane angle curve (adapted from [8])

2.2. Clock Synchronisation Protocols

The synchronisation of all network components clocks plays a critical role in achieving high service efficiency between systems. Having the Instrumented Knee Pads (IKPs) synchronised was crucial for this work because the IKPs start with no time reference. The data obtained from each IKP cannot be established in the same timeline without being in sync.

There are several synchronisation mechanisms. The most common ones are the Simple Network Time Protocol (SNTP), Network Time Protocol (NTP) and Precision Time Protocol (PTP). The PTP protocol is the most precise, achieving clock accuracy in the range of nanoseconds, whereas the SNTP protocol is the least exact [9].

2.2.1. Network Time Protocol

The most widely used and accepted method for maintaining accurate time across entire networks is an implementation of the Network Time Protocol (NTP). NTP is one of the Internet's oldest and most widely used protocols, based on the Internet Protocol (IP) and the User Datagram Protocol (UDP). Even when utilised across typical Internet channels containing several gateways and unstable networks, it is specially intended to preserve time accuracy and reliability [10].

NTP is not founded on the idea of synchronising machines with each other. It is based on the idea that all devices should come near the correct time - Universal Coordinated Time (UTC) [10]. The NTP protocol is used to achieve clock synchronisation between a trusted time server and its clients [10] [11]. Each client runs a small program that regularly contacts the server for an exact UTC reference as a background operation. These queries are run at predetermined intervals (usually every 15 minutes) to ensure that the network maintains the required synchronisation accuracy [10]. On a Local Area Network, without too much network equipment such as switches and routers, it can achieve a precision of tens of milliseconds [11].

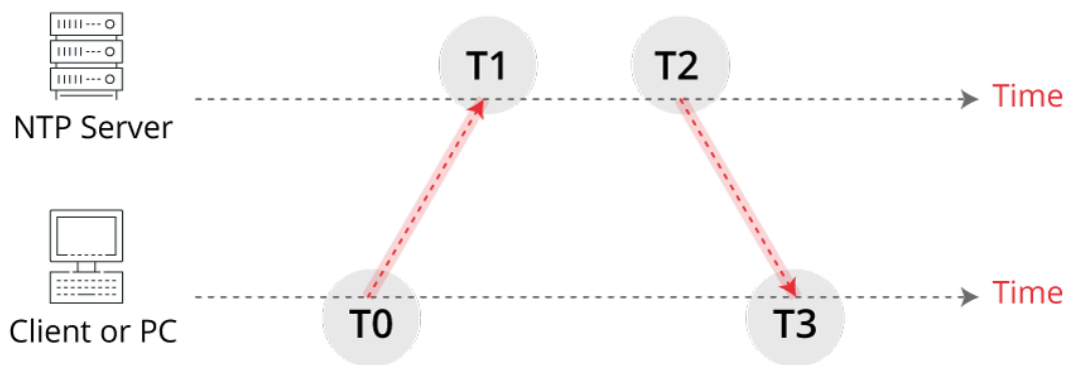


Figure 4: Exchange of messages in the NTP protocol [9]

The fundamental synchronisation idea is that each client sends periodic queries to a group of timeservers, which answer with their own local timestamp. Each client has a list of acceptable servers that is updated regularly. Internal algorithms compare the timestamps from all servers to determine which server has the best stratum and synchronisation distance, which will be used for setting the clock update. The time offset is calculated from a collection of four timestamps (two from the server and two from its own) Figure 4.

A client sends an NTP request message that contains the originate timestamp T_0 (Client Timestamp). Upon receiving the NTP request, the server generates the receive timestamp T_1 (Slave Timestamp). After processing the request, the server sends back to the client the NTP response with the originate timestamp T_2 . The client receives the NTP response and generates the receive timestamp T_3 . The following calculations are performed at the Client and Slave levels.

$$T_1 = T_0 + \mathit{delay}_{CS} + \mathit{offset}_{CS} \quad (2.1)$$

where delay_{CS} is the network delay between client and server and offset_{CS} is the clock offset of the client with reference to the server.

$$T_3 = T_2 + \text{delay}_{SC} + \text{offset}_{SC} \quad (2.2)$$

where delay_{SC} is the network delay between server and client and offset_{SC} is the clock offset of the server with reference to the client.

Adding (2.1) and (2.2) and because $\text{offset}_{CS} = \text{offset}_{SC}$ the round trip delay is:

$$\text{delay}_{CS} + \text{delay}_{SC} = (T_1 - T_0) + (T_3 - T_2) \quad (2.3)$$

Subtracting (2.2) from (2.1) and assuming the same delay, $\text{delay}_{CS} = \text{delay}_{SC}$, the offset is:

$$\text{Offset}_{CS} = \frac{(T_1 - T_0) - (T_3 - T_2)}{2} \quad (2.4)$$

NTP is built on UDP/IP, and its implementation is pure software, timestamps being taken at the application level.

2.2.2. Simple Network Time Protocol

The Simple Network Time Protocol (SNTP) is very similar to the NTP. It is too a TCP/IP protocol that uses the same time packet from a Time Server message to compute accurate time. The difference between SNTP and NTP is the error checking and the actual time correction [9] [12].

The SNTP method is significantly simpler than the NTP method since it usually uses just one Time Server to calculate the time and then “jumps” the system time to the calculated time. It can, however, have backup Time Servers in case one is not available. During each interval, it determines whether the time is off enough to correct and if it is, it applies the correction. The main problem of this protocol is its low security. As it lacks an encryption method, it is vulnerable to attacks in which the time can be modified. So, it is not suggested to utilise the SNTP protocol as a principal source or clock [12].

2.2.3. Precision Time Protocol

The IEEE 1588 standard for Precision Time Protocol (PTP), which was first adopted in 2002 for Automation and Measurement applications, provides a method for clock synchronisation with microsecond accuracy. PTP was also adopted under the IEC 61588 standard in 2004. Version 2 of the IEEE 1588 standard was ratified in 2008 to address telecommunications and audio-video bridging applications.

PTP is in demand wherever processes need to be synchronised precisely, such as automation and control systems, measurement and automatic test systems, power generation, transmission and distribution systems, as well as telecommunications [13].

Unlike NTP and SNTP, in the Precision Time Protocol (PTP), the connection begins with a “server request” [9]. The protocol defines synchronisation messages used between a Master and Slave clock similar to the Server and Client mode used in the Network Time Protocol (NTP). The master is the provider of time, and the slave synchronises with the master. PTP is built over IP and UDP and uses several variables to calculate the offset and delay of a local clock with reference to the master. The protocol uses four messages: *Sync*, *Follow Up*, *Delay Request* and *Delay Response* between a master and slaves. *Sync* and *Delay Request* are used for timestamps, while the other two carry the precise timestamps from the master, respective the slave (

Figure 5).

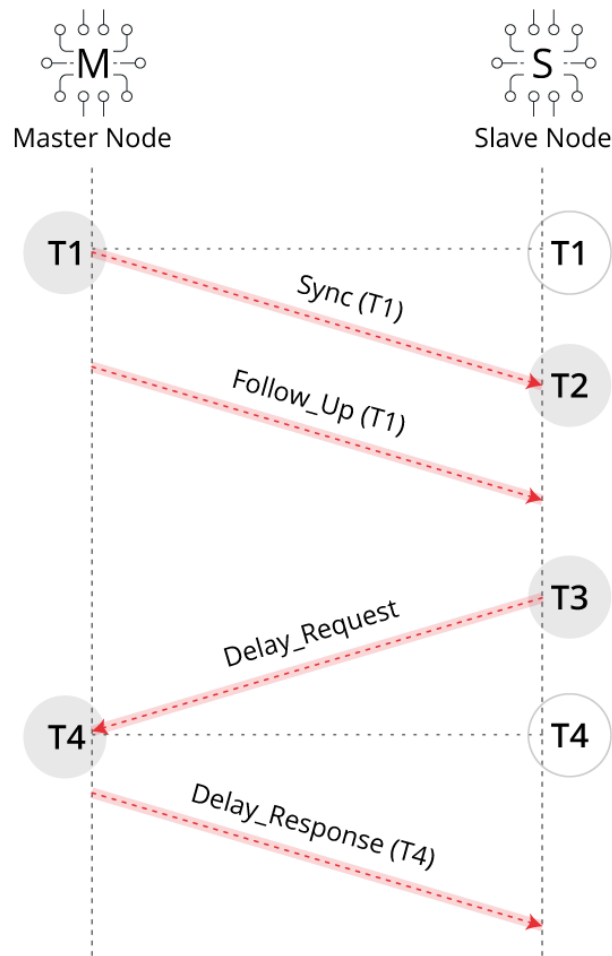


Figure 5: PTP operation [9]

Every slave synchronises to its master's clock by exchanging specific messages. The PTP protocol utilises two phases for setting the local clock (time): Offset measurement phase and Delay measurement phase.

During the Offset measurement, the master periodically transmits sync messages to related slaves using multicasting. The sync message contains the estimated time when the message will leave the master. The master measures the exact time of transmission (Master Time), and the slaves measure the exact time of reception (Slave Time). Optionally, for highly accurate synchronisation, the master can send a *Follow-Up* message that contains the exact time T_1 of transmission of the sync, measured as close as possible to the transmission media. After the first *Sync* and *Follow Up* messages, the slave concludes the following equation:

$$T_2 = T_1 + \textit{offset} + \textit{delay} \quad (2.5)$$

The difference between the slave time T_2 and the master time T_1 is made up of both the *offset* and the *delay*. To determine the *delay*, the slave at time T_3 sends a *Delay Request* message to the master that sends back a *Delay Response* containing the precise time when the *Delay Request* has arrived at the master. As a result:

$$T_4 = T_3 - \textit{offset} + \textit{delay} \quad (2.6)$$

By adding (2.5) to (2.6), *offset* cancels out, and the *delay* can be calculated assuming it is the same in both directions:

$$\textit{delay} = \frac{(T_2 - T_1) + (T_4 - T_3)}{2} \quad (2.7)$$

Now, the *offset* can be calculated on the following *Sync/Follow Up* message exchange:

$$\textit{offset} = (T_2 - T_1) - \textit{delay} \quad (2.8)$$

At this point, synchronisation is achieved by adjusting the time at the slave:

$$\textit{new_slave_time} = \textit{old_slave_time} - \textit{offset} - \textit{delay} \quad (2.9)$$

The *delay* measurement is performed irregularly and at more extensive time intervals than the *offset* measurement in order to reduce the network traffic.

2.3. Human Gait Analysis Related Works

Research into systems capable of analysing human gait has increased and evolved over the years. These works have resulted in a large number of systems and techniques for gait analysis that can be divided into three categories: image processing (IP), floor sensors (FS) and sensors located on the body, carried by the users (wearable sensors—WS) [14]. It was given more relevance to the approaches that can analyse the knee, excluding the floor sensors.

Gait analysis can be carried out through laboratory mounted systems or systems used in an open environment or, in some cases, by combining the two [14].

2.3.1. Image Processing

The typical Image Processing (IP) system consists of multiple digital or analogue cameras with lenses that can be used to gather gait-related information. Techniques such as threshold filtering that converts images into black and white, the pixel count to calculate the number of light or dark pixels, or background segmentation, which removes the image's background, are just some of the possible ways to gather data to measure the gait variables. This method has been widely studied to identify people by the way they walk.

Within IP methods, one technique has become very important: depth measurement also called range imaging. Depth measurement is a collection of techniques used to calculate and obtain a map of distances from a viewpoint. These techniques make it possible to obtain essential image elements with a better and faster real-time process. Several technologies can be applied for this purpose (Figure 6), such as camera triangulation (stereoscopic vision), laser range scanner, and Time-of-Flight methods. Other studies use structured light and infrared thermography.

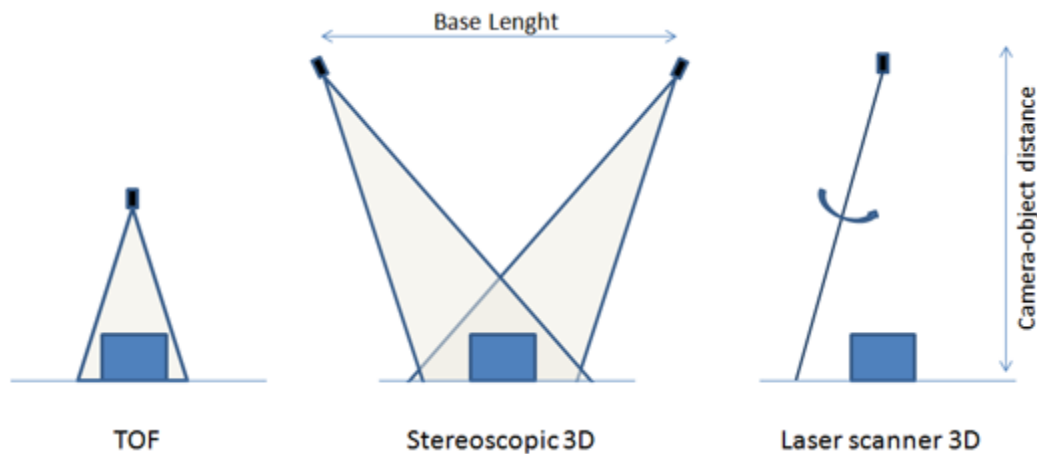


Figure 6: Different technologies for IP based measurement [14].

2.3.1.1. Stereoscopic Vision

Stereoscopic vision can determine the depth of points in a scene, for example, from the midpoint of a line to their focal points. In order to solve the problem of depth measurement using a stereo camera system, it is necessary to first find corresponding points in different images. This technique is based on creating a system by calculating similar triangles between the optical sensor, the light-emitter, and the object in the scene. Creating a camera system involves acquiring multiple images, usually of a calibration grid, in multiple planes. This technique is widely used for gait analysis [15] [16].

2.3.1.2. Time-of-Flight Systems (ToF)

ToF systems are based on cameras using signal modulation that measure distances based on the phase-shift principle [17] (Figure 7). The observed scene is illuminated with modulated near-infrared light, whereby the modulation signal is assumed to be sinusoidal with frequencies in the order of some megahertz. The reflected light is projected onto a charge-coupled device or complementary metal-oxide-semiconductor sensor or a combined technology. The phase shift, which is proportional to the covered distance, is measured in parallel within each pixel [18].

ToF systems were utilised by Derawi et al. to recognise human gait by extracting gait characteristics from various joints and body segments [19].

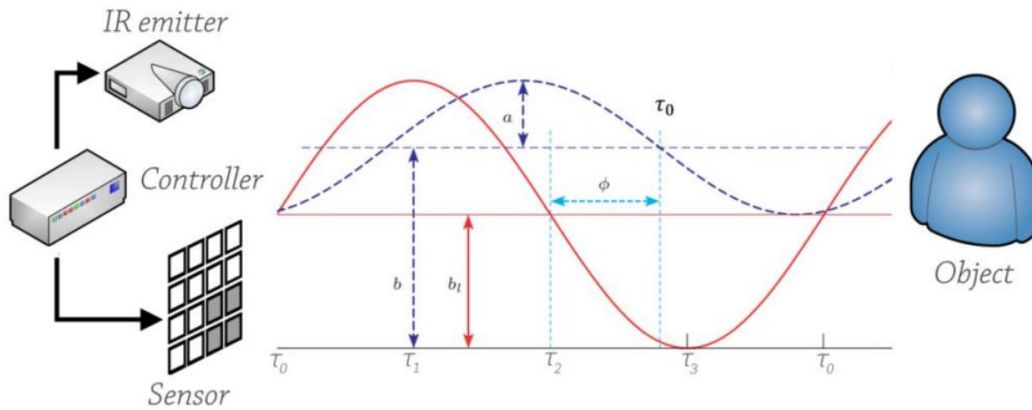


Figure 7: Time-of-flight working principle [14].

2.3.1.3. Laser Range Scanner

The Laser Range Scanner measures a distance by shooting a laser beam towards an object, measuring how long it takes to bounce back. The distance can be figured out by knowing the speed of light (laser beam) and measuring the time [20].

Moreover, using a scanning plane parallel to the ground and dimensional laser range sensors, this system can detect the displacement of the legs. The position of the legs is estimated by fitting two circles with the laser points that define their contour, and the gait parameters are extracted applying a step-line system to the estimated displacement of the legs to reduce uncertainty in the determination of the stand and swing phase of the gait [21].

The main advantages of using a laser range sensor to register gait are that only one laser sensor placed with the scan plane parallel to the ground is needed to register the displacement of the legs. The laser range sensor allows medium-range walking displacements comprising several strides. No external markers attached to the human body are needed. The system can be used in indoor and outdoor measurements, depending on the laser sensor, and can be used on any ground surface without any visual references. The system does not require initial calibration or reference scales. The measurement system can be mounted everywhere in minutes. The primary drawback of the basic measurement method is that it will only acquire planar information on the position of the legs at a set height. However, several laser range sensors may be utilised to get additional body motion parameters at varying heights described by [21] [22].

2.3.2. Wearable Sensors

Wearable sensors are used in gait analysis to evaluate several aspects of human gait. They are put on various areas of the patient's body, such as the feet, knees, and hips [2] [23]. Gait analysis with wearable sensors has used different motion sensors and systems, such as the accelerometer, gyroscope, magnetoresistive sensors, flexible goniometer, electromagnetic tracking system (ETS), sensing fabric, force sensor, and sensors for electromyography. Based on these sensors, a single type or a combined sensor system of multiple sensors may be used for various gait analysis applications. The basic principles and features of these motion sensors and systems are described in the following.

2.3.2.1. Accelerometer, Gyroscope, and Magnetoresistive Sensors

An accelerometer is a type of inertial sensor that can measure acceleration along its sensitive axis. The typical operation principle of accelerometers is based on a mechanical sensing element that comprises a proof mass attached to a mechanical suspension system to a reference frame. According to Newton's second law, the mass proof can be deflected by the inertial force because of acceleration or gravity (force = mass \times acceleration). Based on this principle, the acceleration can be measured electrically using the physical changes in the displacement of the proof mass with respect to the reference frame. Three common types of accelerometers are available, namely, piezoelectric, piezoresistive, and capacitive accelerometers. Piezoresistive and capacitive accelerometers can provide dual acceleration components and have higher stability. Thus, these accelerometers are suitable for measuring the motion status in the human gait [24]. By attaching these accelerometers to the feet or legs, the acceleration/velocity of the feet or legs in the gait can be determined to perform the gait analysis [25].

A gyroscope is an angular velocity sensor. The micromachined gyroscope is based on the concept of measuring the Coriolis force, which is an apparent force proportional to the angular rate of rotation in a rotating reference frame. The angular rate can be obtained by detecting the linear motion from the Coriolis effort and integrating the gyroscopic signal. In addition, gyroscopes based on other operating principles also exist, such as the electronic, microchip-packaged MEMS gyroscope devices found in consumer electronic devices, solid-state ring lasers, fibre optic gyroscopes, and the extremely sensitive quantum gyroscope. A gyroscope can be applied to measure the motion and posture of the human segment in gait analysis by measuring the angular rate [26] [27]. For example, by attaching a gyroscope to human feet or legs, the angular velocity and angle of feet or legs during the gait can be

determined to reorganise the various gait phases. A gyroscope is usually combined with an accelerometer in the gait analysis to construct a complete initial sensing system.

Magnetoresistive sensors are based on the magnetoresistive effect (Figure 8). If a magnetic flux (magnetic field) is not applied, the current flows straight through the InSb plate. However, if a magnetic flux is applied, a Lorentz force proportional to the magnetic flux density will deflect the current path.

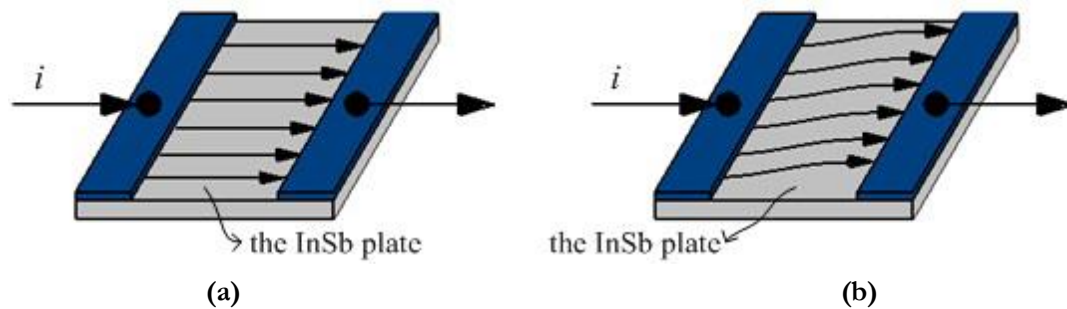


Figure 8: The model of magnetoresistive effect. (a) current mode under non-magnetic field; (b) current mode under magnetic field [2].

As the current path is deflected, the current flows through the plate for a longer distance, causing the resistance to be increased. The magnetoresistive effect refers to the change in the resistivity of a current-carrying ferromagnetic material resulting from a magnetic field, with the resistance change proportional to the tilt angle in relation to the magnetic field direction. Based on this magnetoresistive effect, magnetoresistive sensors can estimate changes in the orientation of a body segment in relation to the magnetic North or the vertical axis in the gait analysis [28]. Such sensors can provide information that cannot be determined by accelerometers or the integration of gyroscope signals.

2.3.2.2. Flexible Goniometer

Unlike the inertial sensor, the flexible goniometer is operated by measuring the change in the physical signal resulting from the angular change. A flexible goniometer can be used to measure the relative rotation between two human body segments. The flexible goniometers used in gait analysis can be divided into strain gauges, mechanical flexible, inductive, and optical fibre goniometers [2]. Several flexible electrogoniometers based on a strain gauge have been developed and used for angle measurement in gait analysis. At present, numerous commercialised flexible electrogoniometers are available for the measurement of human posture and spinal motion [29]. A mechanical flexible goniometer is designed to obtain angular change by measuring the longitudinal displacement of two parallel wires bent

in the plane of rotation, which is demonstrated by measuring the knee joint during human walking [30] [31].

2.3.2.3. Electromagnetic Tracking System (ETS)

Based on Faraday's law of magnetic induction, the electromagnetic tracking system (ETS) is a type of 3D measuring instrument [32]. When a sensor coil-carrying item moves within controlled magnetic fields, the induced voltages in the sensor coils vary in proportion to the change in the object's position and orientation relative to the source of controlled magnetic fields. The regulated magnetic fields in the ETS are created by a stationary transmitter and sensed by receivers mounted on the moving item. As a result, the object's positions and orientations in relation to the transmitter may be determined. Some developed marketed ETSs have been used in bioengineering, such as gait analysis and the kinematic research of body segments, based on this operating concept [33] [34].

3. Developed System

At the beginning of this work, we decided to focus on the Knee Sagittal Plane Angle Curve (KSPAC) to study and analyse the human gait. For that, two Instrumented Knee Pads (IKPs) were developed with different ways of measuring the KSPAC. One IKP is based on an absolute encoder, and the other uses two IMUs.

To read and collect the IKPs sensors data, was used a mini microcontroller board with Wi-Fi. Each IKP microcontroller synchronises its clock with the other leg IKP microcontroller via wireless before sending the collected data to a computer with a Windows Forms Application (WFA) developed to save and process the data in these two systems.

3.1. Encoder Instrumented Knee Pad

3.1.1. Hardware Selection

In the first IKP system, we opted for an encoder to measure the KSPAC because these sensors generate digital signals to quantify an angle. It was chosen a rotative encoder because it responds to the rotation and measures the angular velocity and acceleration.

In general, there are two main types of encoders: incremental and absolute. Incremental encoders generate a series of pulses in response to motion and can measure speed or, via a counter, to track position. On the other hand, absolute encoders generate multi-bit “digital words” that directly indicate the actual angular position. A significant benefit of absolute encoders is that if the device’s power supply is interrupted, the device “saves” its position [35], and for that reason, was selected an absolute encoder.

The first step in selecting the hardware was to select a low-cost rotary encoder. For this project, the encoder needed to have high precision, be absolute, compact, have low power consumption and be immune to noise and dirt due to being placed in a structure where there is a constant movement of the hardware.

Given the needs presented, the best solution was the CUI-AMT222B encoder (Figure 9), a capacitive modular encoder, with 14 bits of resolution, with an operating temperature from $-40\text{ }^{\circ}\text{C}$ to $+125\text{ }^{\circ}\text{C}$, easy to install and costing about 45€ [36].

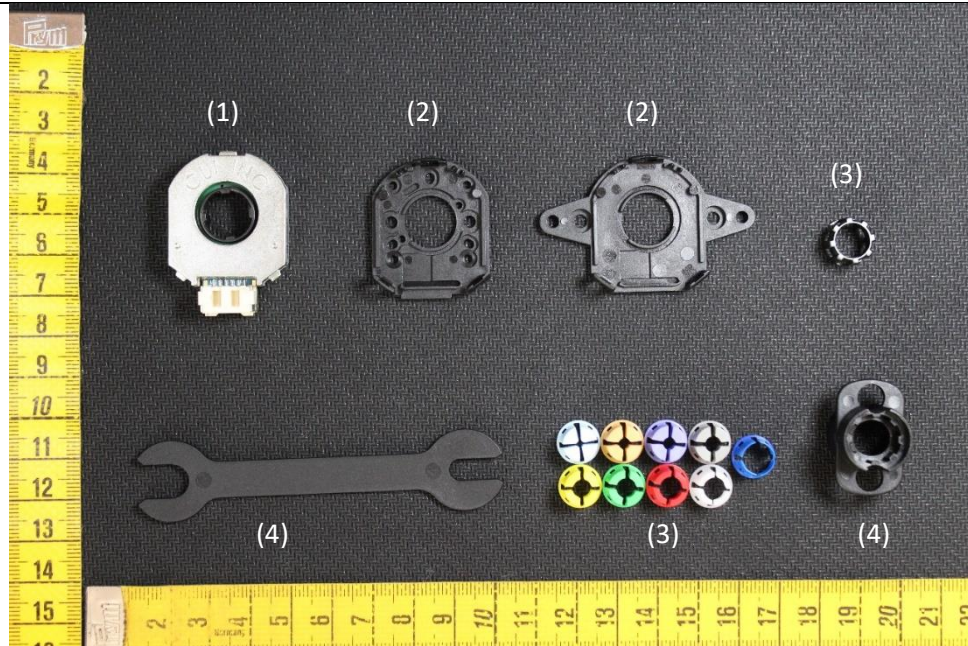


Figure 9: CUI-AMT22 pack: (1) CUI-AMT22 encoder, (2) holding back cases, (3) centre fixing pieces, (4) mounting tools

3.1.2. System Assembly

3.1.2.1. System Structure

This system uses two hinged rigid structures and is placed at the back of the leg. The system consists of two rigid plastic structures (RPS), one for the thigh and the other for the calf, joined by a central metallic axel, as shown in Figure 10.

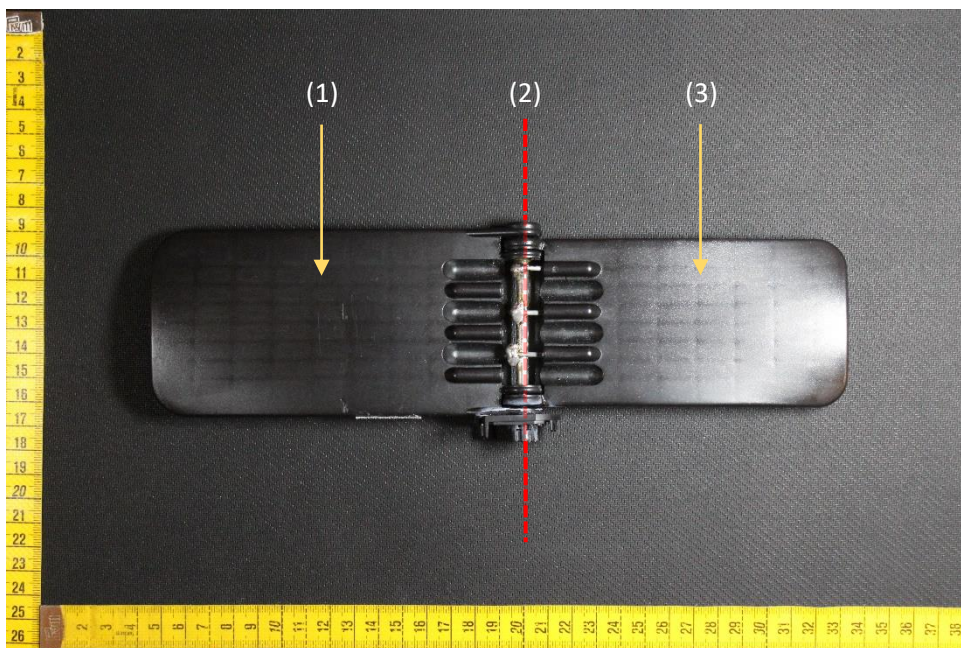


Figure 10: (1) Thigh RPS, (2) central axel, (3) calf RPS

The Knee Sagittal Plane Angle (KSPA), the angle between the two RPS, is measured by the rotative encoder, linked with its central part to the axel and the outer case held to the thigh RPS (see APPENDIX for more constructive details).

3.1.2.2. Connections Scheme

In order to read and collect the encoder angles captured while using the Instrumented Knee Pad (IKP), the encoder was connected to a microcontroller with Wi-Fi. We have based ourselves on the ESP8266 modules because this microcontroller has low prices, small dimensions, and three development environments available: Lua, Arduino and RTOS, selecting the Wemos D1 mini-board, as shown in Figure 11. The Wemos D1 mini-board uses a microcontroller (ESP-12) that contains 4 MB flash memory, making it possible to exploit all the ESP8266 features, has a USB converter and a voltage regulator. The most significant advantage of this device is its low price and reduced dimensions, almost half the size of the NodeMCU board, which reduces the number of GPIO ports to 8, sufficient for this project. The connections between the devices are presented in Table 1.

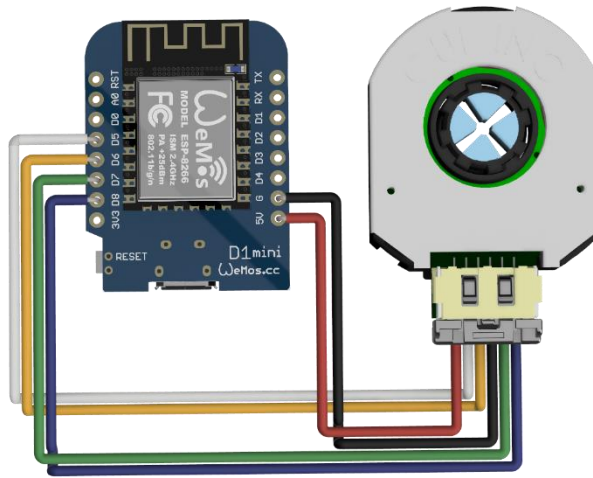


Figure 11: Scheme connections between encoder and Wemos D1 mini board

Table 1: Pin connections between encoder and Wemos D1 mini board

Function	Encoder Pin Number	Wemos D1 mini	Wire colour
+5V	1	5V	Red
SCLK	2	D5	White
MOSI	3	D7	Green
GND	4	GND	Black
MISO	5	D6	Yellow
CHIP SELECT	6	D8	Blue

3.1.3. Software measuring system

After the hardware have been selected and assembled, a C++ code was developed (see APPENDIX B), which uses a function adapted from a sample of CUI Devices [37] that, when called, reads the instant angle. This function gets the absolute position from the AMT22 encoder using the SPI bus. The AMT22 position includes two check bits for position verification. Both 12-bit and 14-bit encoders transfer position via two bytes, giving 16-bits regardless of resolution. For 12-bit encoders, the position is left-shifted two bits, leaving the right two bits as zeros. This shifting gives the impression that the encoder sends 14-bits when it sends 12-bit values, where every number is multiplied by 4. This function takes the pin number of the desired device as an input as well as the encoder resolution, expecting res12 or res14 to properly format position responses. Error-values are returned as 0xFFFF.

3.2. IMU Instrumented knee pad

3.2.1. Hardware Selection

The second system to measure the Knee Sagittal Plane Angle Curve (KSPAC) developed for this project uses an Inertial Measurement Unit (IMU). For the IMU Instrumented knee pad, was selected the MPU6050. This device is a Micro Electro-mechanical system, consisting of a three-axis accelerometer and three-axis gyroscope, with a 16-bit analogue-to-digital converter for each channel, which allows calculating the angle for each axe. Using two of these sensors, placed at the front of the thigh and shin, as shown in **Error! Reference s**

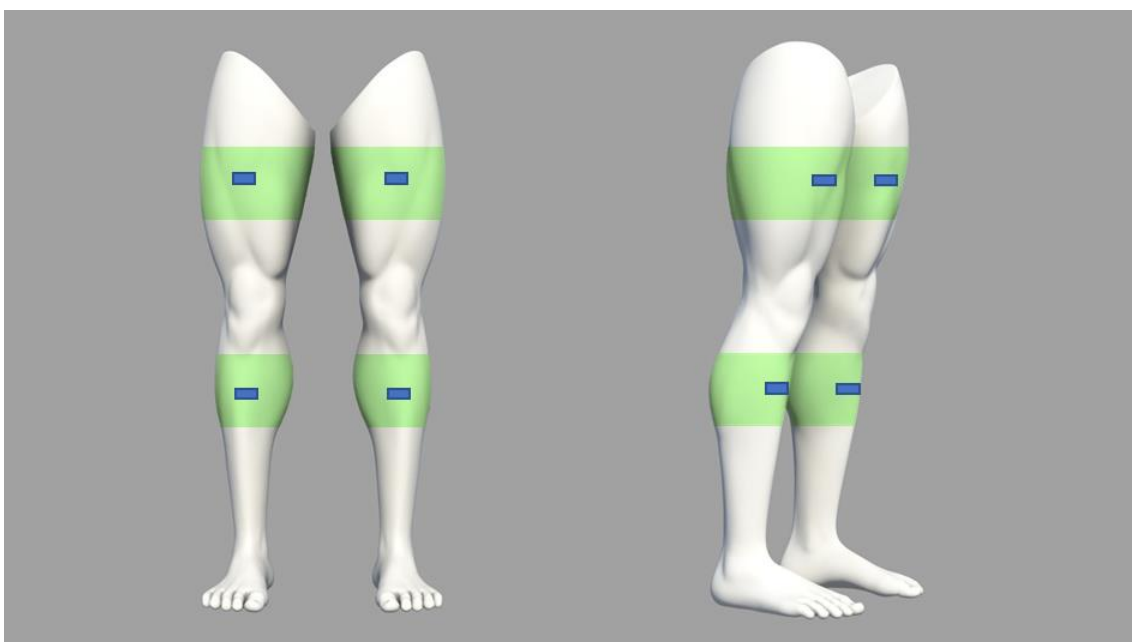


Figure 12: IMU instrumented knee pad - placement

ource not found., the Knee Sagittal Plane Angle (KSPA) can be calculated by making the difference between the two obtained angles from the sensors in the sagittal plane of the leg.

3.2.2. Connections Scheme

As well as in the Encoder IKP, the IMU was connected to a Wemos D1 mini-board, as shown in Figure 13. The connections between the devices are presented in Table 2.

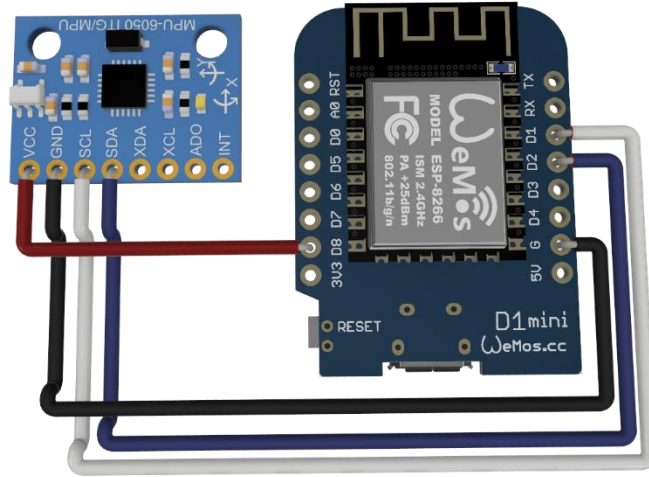


Figure 13: Scheme connections between IMU and Wemos D1 mini board

Table 2: Pin connections between IMU and Wemos D1 mini board

Function	IMU Pin Number	Wemos D1 mini	Wire colour
VCC	1	D8	Red
GND	2	GND	Black
SCL	3	D1	White
SDA	4	D2	Blue

3.2.3. Software measuring system

The MPU6050_light.h library was used for the IMU system to get the raw data coming from MPU6050. We started with a calibration routine that averages the first ten readings to compute the default sensor offsets. The angle for each x, y and z axes was then calculated from the raw values of the accelerometer and gyroscope [38].

Both the accelerometer and gyroscope data are prone to systematic errors. The accelerometer provides accurate data over the long term but is noisy in the short term. Moreover, the gyroscope provides accurate data about changing orientation in the short term, but the necessary integration causes the results to drift over longer time scales.

The solution to these problems is to fuse the accelerometer and gyroscope data to cancel out the errors. It was used a simple approximation for combining these two data types, called Complementary Filter. In its most simple form, the filter looks as follows:

$$\text{Filtered Angle} = \alpha \times (\text{Gyro Angle}) + (1 - \alpha) \times (\text{Acc Angle}) \quad (3.1)$$

$$\alpha = \frac{\tau}{(\tau + \Delta t)} \quad (3.2)$$

$$\text{GyroAngle} = \text{LastMeasuredFilteredAngle} + \omega \times \Delta t \quad (3.3)$$

where the **GyroAngle** is the computed filtered gyroscope angle, Δt is the sampling rate, and τ is the time constant greater than the timescale of typical accelerometer noise.

We had a sampling rate of 10 milliseconds and chose a time constant of about 0.1 seconds, giving $\alpha \approx 0.91$.

3.3. Instrumented Knee Pads Synchronisation and Data Transferring

After having the two systems assembled, data was sent to the computer every ten milliseconds at a frequency of 100Hz. The computer application then collected this information. For the data transferring process, we ended up with two solutions:

- Through a local Wi-Fi network using a TCP/IP protocol, the Instrumented knee pads were connected to the same network as the computer;
- Connect the computer with a Wemos D1 mini-board via a serial port, which communicates with the other boards in the Instrumented knee pads using the ESP-NOW protocol.

In the first solution for the data transferring process, it is needed to individually connect the two IKPs to the local Wi-Fi network. Each IKP on the first boot will be in **set up station mode**, read the pre-registered SSID and password combinations, and try to connect to the same. If this process fails, it sets the IKP into **Access Point mode**. It creates an open Wi-Fi (not protected with a password), named “KneePads – Left/Right”. This open Wi-Fi will allow the user to connect using any Wi-Fi enabled device with a browser or a computer with the developed application. After establishing a connection with the IKP Access Point, opening a browser with the Wemos board default IP address, 192.168.4.1, shows a web page that allows the user to configure the SSID, the password and the computer ID. If the developed application is used to configure the SSID, password and computer ID, open in

Settings>New Wi-Fi Connection, as shown in Figure 14 (more visual information in APPENDIX C).

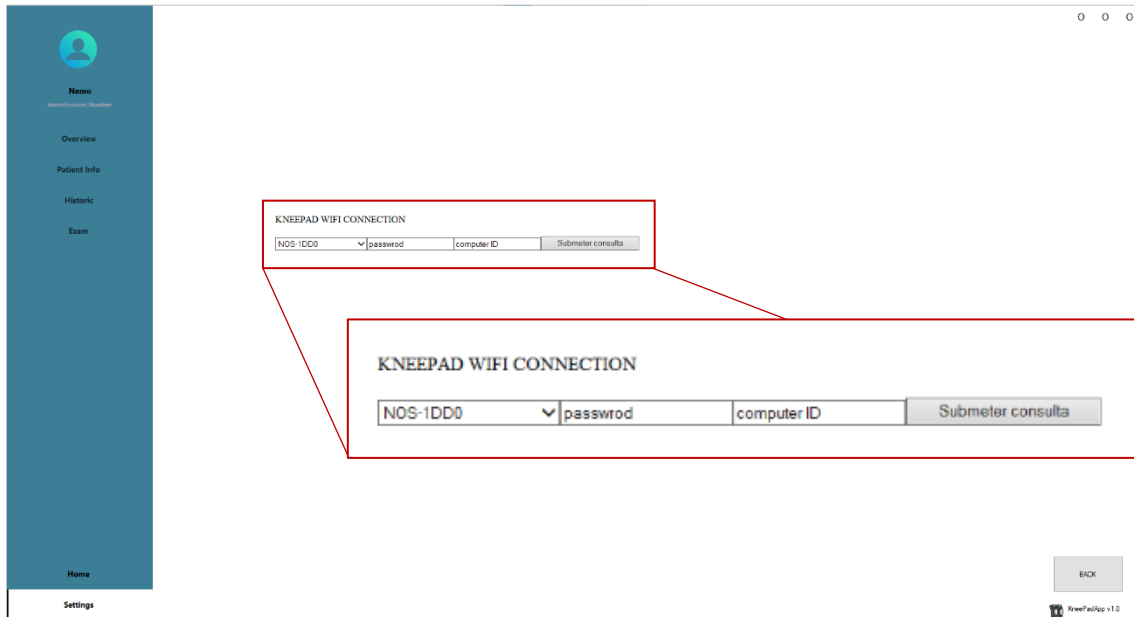


Figure 14: Stablish new Wi-Fi connection through the developed application

Once a new SSID and password are set, the IKP reboots and tries to connect. If it establishes a connection, the process is completed successfully. If the connection fails, it will be set up again as an Access Point to configure the new SSID and Password.

After connecting the IKPs to the local Wi-Fi network where the computer is connected, the information is passed through a TCP/IP protocol. The computer behaves as the server and the IKPs as the client.

In the second solution for the data transferring process, a Wemos D1 mini-board was connected to a computer with the developed application via a USB serial port. This board communicates with the other boards in the Instrumented knee pads using the ESP-NOW protocol.

The ESP-NOW is a fast communication protocol that can be used to exchange small messages (up to 250 bytes) between ESP8266 boards, enabling multiple devices to communicate without using Wi-Fi. The protocol is similar to the low-power 2.4GHz wireless connectivity that is often deployed in wireless mice. So, the pairing between devices is needed before their communication. After the pairing is done, the connection is secure and peer-to-peer, with no handshake being required. This means that after pairing a device with each other, the connection is persistent. If suddenly one of the boards loses power or resets, it will automatically connect to its peer to continue the communication when it restarts.

In both data transferring processes, for the user to start collecting new information, he needs to open the application in “Exam”, choose a Trial type, click on the ADD TEST button to open the connections and click on the START button to begin the exam. After starting the exam, the computer exchanges messages with each Instrumented knee pad (IKP) to synchronise the clocks using the Precision Time Protocol (PTP). After all the clocks are synchronised, the computer sends a message to begin the collection of data. When the user has collected enough data, he just needs to click on the STOP button, and the exam ends. Right next, a window pops asking if the user wants to save or not the collected data.

After studying and implementing these two solutions, we end up choosing the ESP-NOW strategy. This choice was made based on the easy use of this solution, being almost a “plug and play” method for the user. This method just needs to connect the Wemos D1 mini-board to a computer via a USB port, switch on the Instrumented knee pads, and start the exam using the application.

3.4. Developed Application

To communicate with the Instrumented knee pads, a Windows Forms Application (WFA) was developed based on the C# language built in the Visual Studio program. When opening the develop application, the user can select an existing patient at the main page and “Login”, add a new patient or go to the “Settings” page. On the “Settings” page, the language between Portuguese and English can be switched, changed the app’s colour style, and Export or Import the patients’ database to/from an excel datasheet.

After selecting a patient and “Login”, four pages about the patient are enabled: “Overview”, “Patient Info”, “Historic”, and “Exam”, as shown in Figure 15.

The information about the patient exams data is presented on the Overview page, divided into four subpages: Measures, Reference, Compare Knees and Report.

- Measures – show all the exams done by the patient, organised by date, test type, and the trial number.
- Reference – exhibit the calculated values from collected data, as the maximums and minimum values, the gait mean velocity and the average gait percentage inside the norm value band from the literature.
- Compare Knees – gives a comparison between the two knees maximums and minimums and presents the angular and time asymmetry.

- Report – has each step values presented on a table which can be saved to a generated report in “.pdf” format with all patient tests’ information.

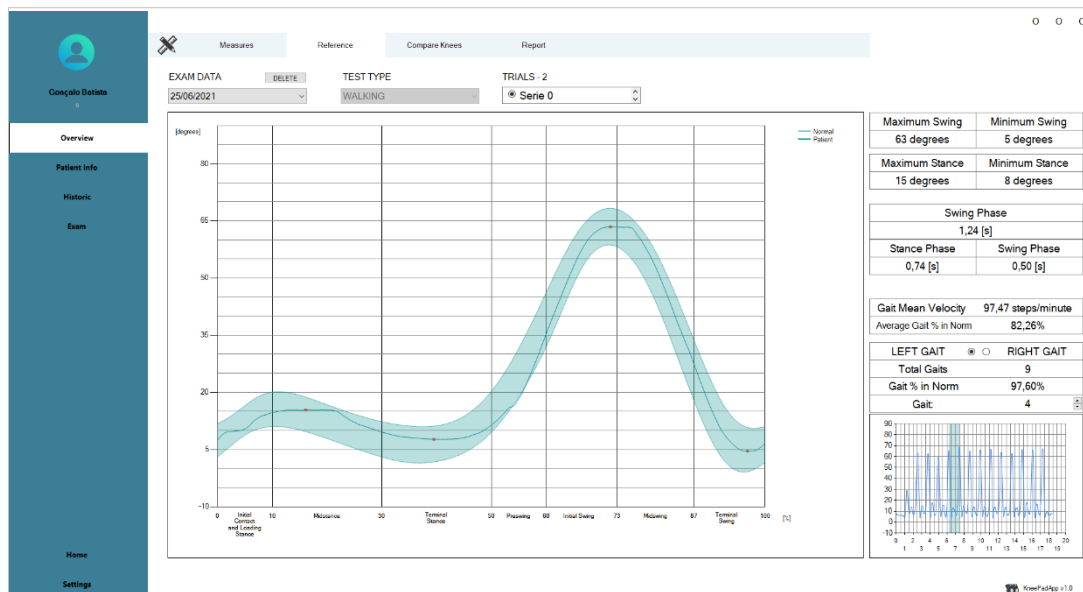


Figure 15: Patient Overview>Reference subpage

The Patient Info page presents all personal information about the patient, which can be edited if some data is wrong or needs actualisation.

On the Historic page, there is a calendar that marks each patient exam date. Selecting a date shows all the information about that exam, like the session hour, session type, affected side knee, and the number of trials. Further observations written by the doctor and the Knee Outcome Survey filled by the patient are also presented. [39]

By opening the Exam page, the user can start a new trial exam. On this page, the Session type, the Affected side, some observations during the exam by the doctor, and the Knee Outcome Survey filled by the patient can be noted.

More interface layouts of the developed Application is shown in Appendix C.

3.5. Instrumented Knee Pad Powering System

To power the IKP systems, were used 5000 mAh power banks, individually connected to each Wemos D1 mini-board with a micro-USB cable. Using these small 9.1×3.7 ×2.2 cm power banks makes it possible to use the IKP system constantly, swapping out the power banks when they are empty, without the need of restarting the system. Since the IKP system has a low power consumption, it allows 31 hours of constant use (maximum time duration in a real experience).

4. Tests and Results

After all the hardware and software concluded, some tests were run to validate the system. Before doing any test, some procedures have to be followed, like placing the IKPs in the legs, establishing the type of soil, footwear and space and time to walk.

4.1. Exam Procedure

The first step is to place the Instrumented knee pads in the patient legs, well adjusted. For both systems, Encoder and IMU, the patient needs to be well seated with the tights out of the seat.

In the Encoder IKPs, the patient needs to place the central joint of the rigid structure in the back of the leg and bend the knee, as shown in Figure 16.



Figure 16: Placing encoder instrumented knee pad on the patient leg

Next, as shown in Figure 17, the patient tightens the thigh straps first (1) and then the calf straps (2).



Figure 17: Encoder instrumented knee pad holding straps

Figure 18 shows the encoder instrumented knee pad, all set up in a walking test.

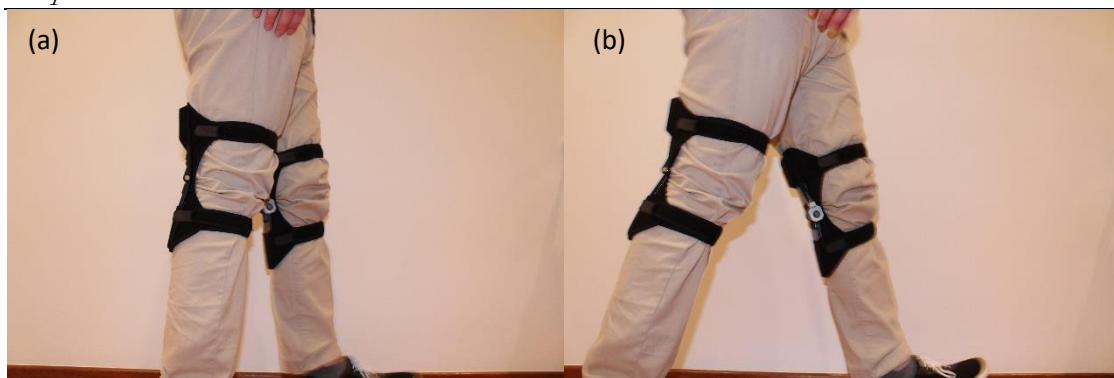


Figure 18: After setting up the encoder knee pads: (a) standing, (b) walking

In the IMU Instrumented knee pads system, the patient needs to place the fabric straps in the thigh and shin with the IMUs holding cases oriented on the front side of the leg and the power banks on the lateral side of the leg (Figure 19).



Figure 19: a) front side of the leg, b) lateral side of the leg

After the patient has positioned the two fabric straps in the leg, the IMUs must be aligned one with the other, the patient standing with the feet shoulder-width apart, by using a pendulum, as shown in Figure 20. The white vertical marks on the fabric straps have to be aligned with the pendulum white string.



Figure 20: (a) Marks for alignment on the fabric straps, (b) pendulum align IMU instrumented knee pad

After the previous steps to place the IKPs and the software application is opened in the “Exam page” the system is ready to start a test.

The various tests done in the course of this thesis were conducted in two specific environments:

- Environment A - closed hallway with a tile floor;
- Environment B - open-air tarmac road.

These two environments were chosen in order to allow the patient to walk in a straight line during the several tests.

For the experiment, we conducted tests on nine people using trainers. Of these people, all nine have done 10 meters walking tests in Environment A, and only one person has done 2-minute and 6-minute walking tests in Environment B.

4.2. Data Processing

In order to analyse the tests carried out by the patient before the final data is dispatched to the user on the Overview subpages, the program processes the raw data. For this, was developed a Matlab function (APPENDIX B) added in a .dll file that the Windows Forms Application can execute, which:

- Calculates the gait time in a hundred per cent;
- Select the chosen gait angles;
- Select the chosen gait times;
- Shows the total gaits;
- Calculates the gait maximum Swing;
- Calculates the gait maximum Stance;
- Calculates the gait minimum Swing;
- Calculates the gait minimum Stance;
- Calculates the percentage of the selected gait points inside the norm value band from the literature.

After the collected data is processed, the information is presented to the user on the Overview page (OP).

By selecting the OP, the automatic subpage that is shown is the Measures subpage. On this subpage, the time scale from the measuring data is changed from milliseconds to seconds and removes the first data values captured before the walking experiment.

If selected the Reference subpage, where the captured values are compared to the standard values from the literature, the Matlab script starts cutting the total gait analysis in individual gaits. This division is based on each gait time, calculated by the difference between the maximum values of consecutive Swing phases. The gait time is then converted into a percentage, knowing that the maximum Swing phase value corresponds to the 72% position in the gait. Besides the maximum Swing phase value, the maximum and minimum values and the time for each gait cycle's Stance and Swing phases are also identified. In addition, the gait mean velocity is calculated by counting the number of gait cycles in the total time, in steps per minute, and checking the percentage of the gait values between the literature values for validation.

The Compare Knees subpage shows the maximum and minimum values for each knee and the angular and time asymmetry, calculated as suggested by Walter Herzog *et al.* [40]:

$$SI = \frac{X_R - X_L}{\frac{1}{2}(X_R + X_L)} \times 100 \quad (4.1)$$

where X_R is a gait variable recorded for the right leg and X_L is the corresponding variable for the left leg.

4.3. Results and Discussion

Some verification tests were done to prove that the Instrumented knee pads systems are measuring values correctly while moving.

For the Encoder IKP, was fixed a protractor to the thigh structure and put a red marker in the calf structure. Then, sitting and standing up movement was repeated (Figure 21) to check whether the values obtained in the application and by observation through the protractor presented the same difference after constant movements to quantify the Encoder IKP measuring error. The results curve is presented in Figure 22, and the values obtained from the experiment are presented in Table 3. We find that the encoder IKP has a slight deviation when used, reaching accuracy with an error of fewer than ± 1 degree.

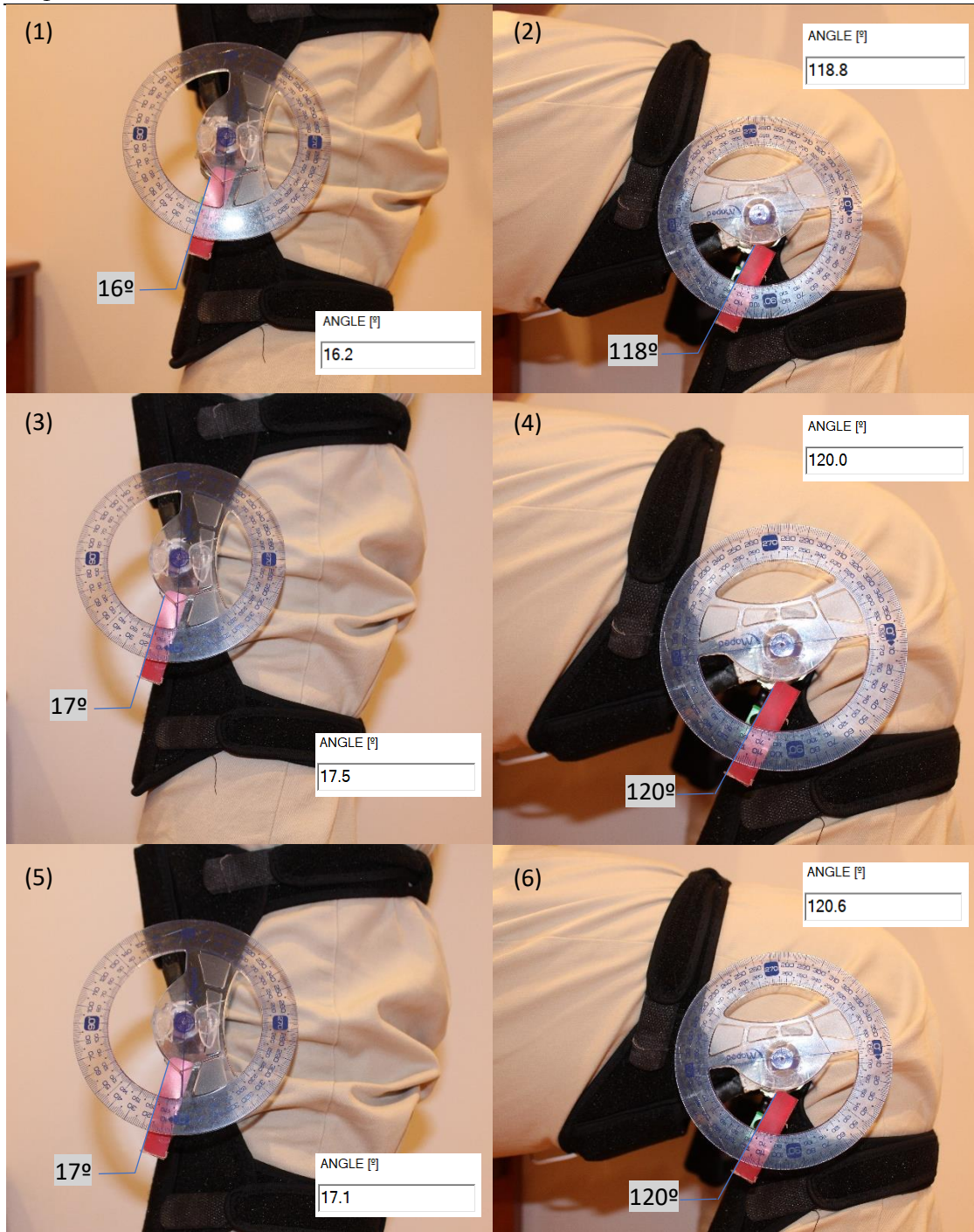


Figure 21: Verification of the Encoder IKP collected values vs measured protractor values
(1) first stand, (2) first sit, (3) second stand, (4) second sit, (5) third stand, (6) third sit.

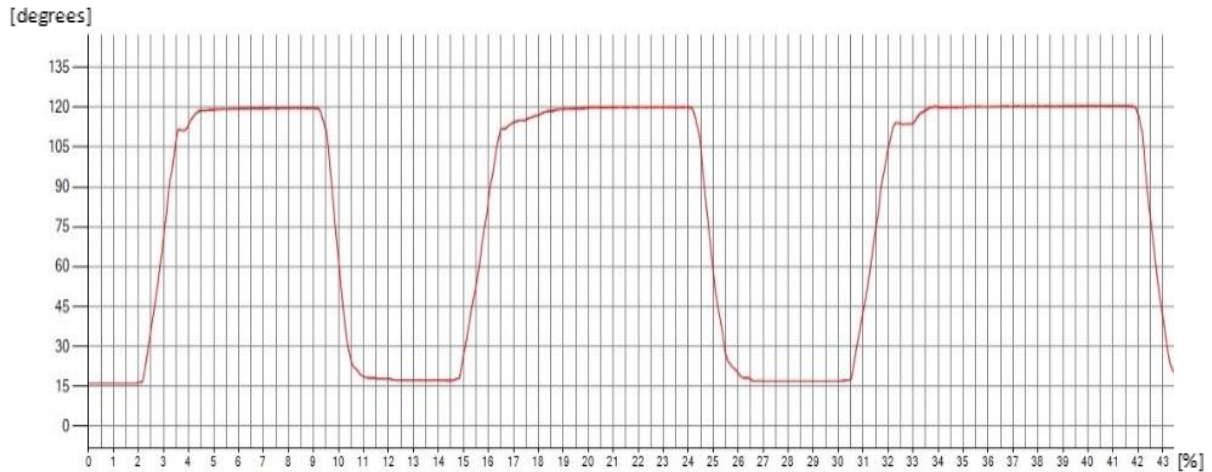


Figure 22: Sitting and standing up IKP movement curve

Table 3: Sitting and standing up movement readings – IKP and protractor

	First stand [degrees]	First sit [degrees]	Second Stand [degrees]	Second Sit [degrees]	Third Stand [degrees]	Third Sit [degrees]
Average readings IKP	16.2	118.8	17.5	120.0	17.1	120.6
Protractor readings	16	118	17	120	17	120

With the IMU Instrumented knee pad, were done different tests. The IMU IKP, when in place at the thigh and shin, the base values are different from person to person because of the volumetry of each person’s legs. Due to this, the IMUs were assembled to a measuring structure, enabling comparing the measured values with the IMUs and by observation. Each IMU (thigh and shin) was assembled to the structure’s arms, allowing the visual protractor and the IKP measurements simultaneously to the same angle. The experiment repeated the movement of the zero position to a fixed value position. After measuring different angles, we found that the IMU IKP has reasonable values when the consecutive angle measures have small amplitudes, with an error less than ± 1 degree, Figure 23. On the other hand, when the consecutive amplitudes are more significant, the error reaches a difference of ± 3 degrees, Figure 24.

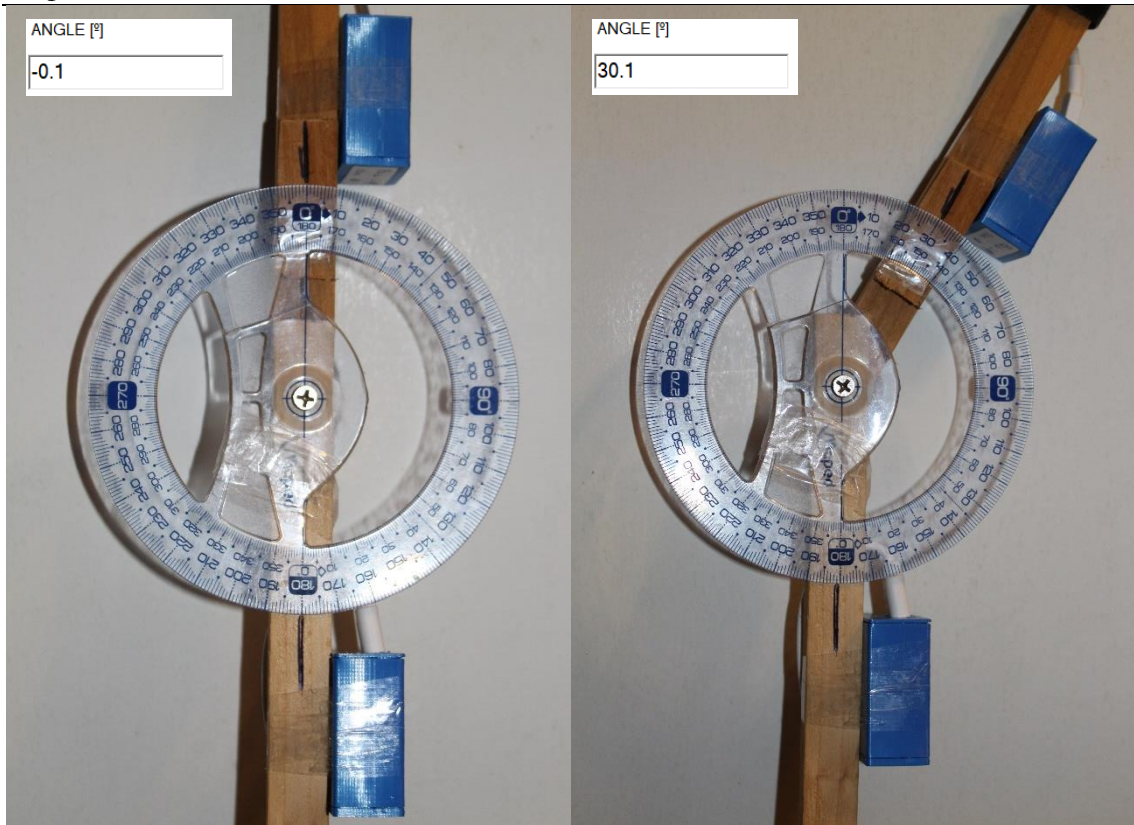


Figure 23: Verification of the IMU IKP collected values vs measured protractor value – (1) 0°, (2) 30°.



Figure 24: Verification of the IMU IKP collected values vs measured protractor values – (3) 60°, (4) 90°.

After verifying the measures of the two IKP systems, the next step was to know the viability of the systems in acquiring values to analyse the knees. Thus, we conducted tests with the two IKPs (Encoder and IMU) in a healthy person in environment A (closed hallway

Chapter 4. Tests and Results

with a tile floor) with the following procedure: two squats > 10 meters walking > more two squats. The squats in the beginning and end are to synchronise the Encoder IKP with the IMU IKP for the same test and to compare the curves obtained from the two systems. From these tests, were obtained the curves for the two knees shown in Figure 25.

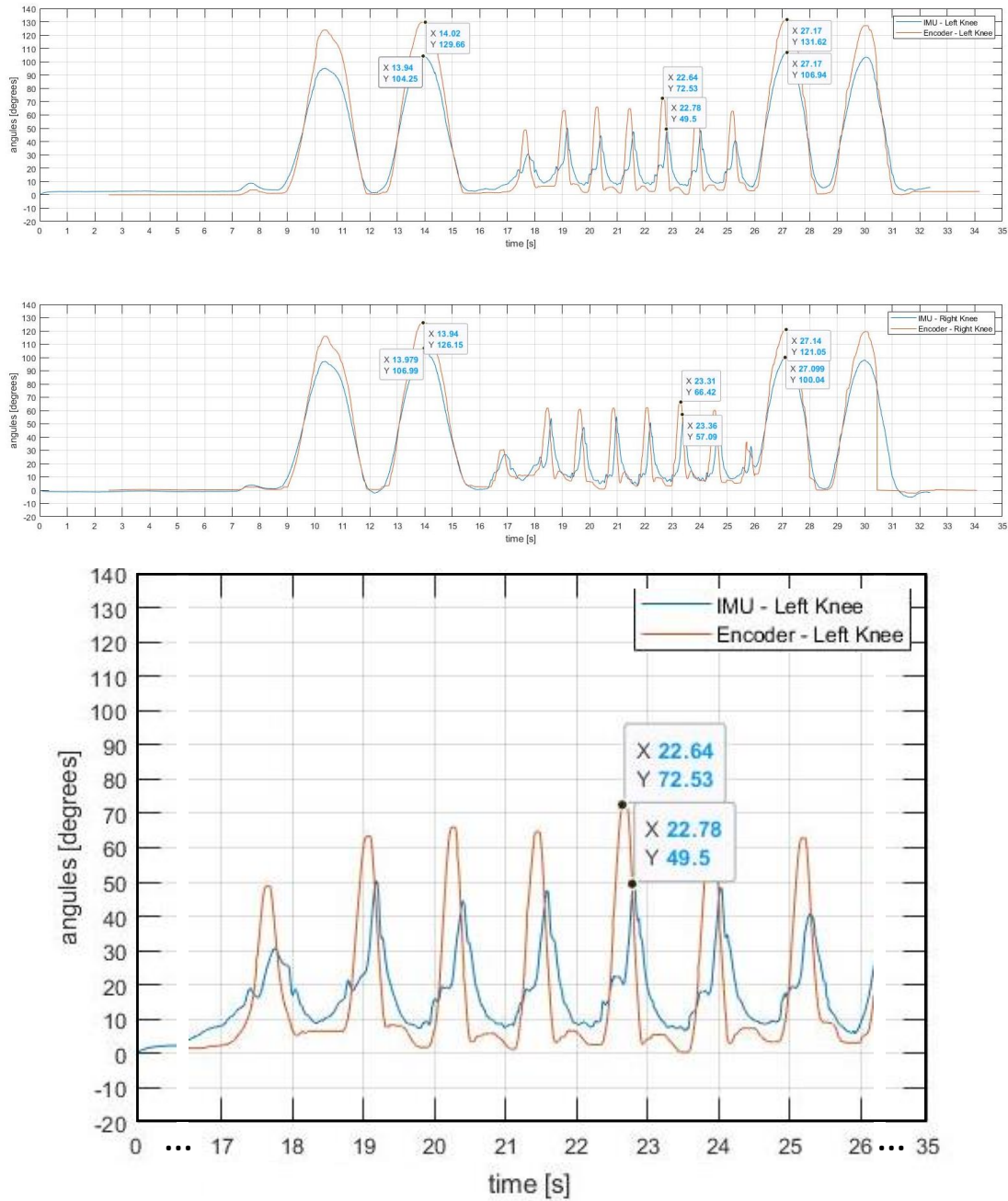


Figure 25: Encoder and IMU IKPs gait curves from 10 meters walking test

As can be observed, the two systems curves are different. The curves were compared to the normal band curve [41] to determine the most accurate. The best walking gait curve was picked from each IKP system, resulting in the charts below. Figure 26 is the best curve

[degrees]

Chapter 4. Tests and Results

recorded with the Encoder IKP system, demonstrating the technology's excellent performance.

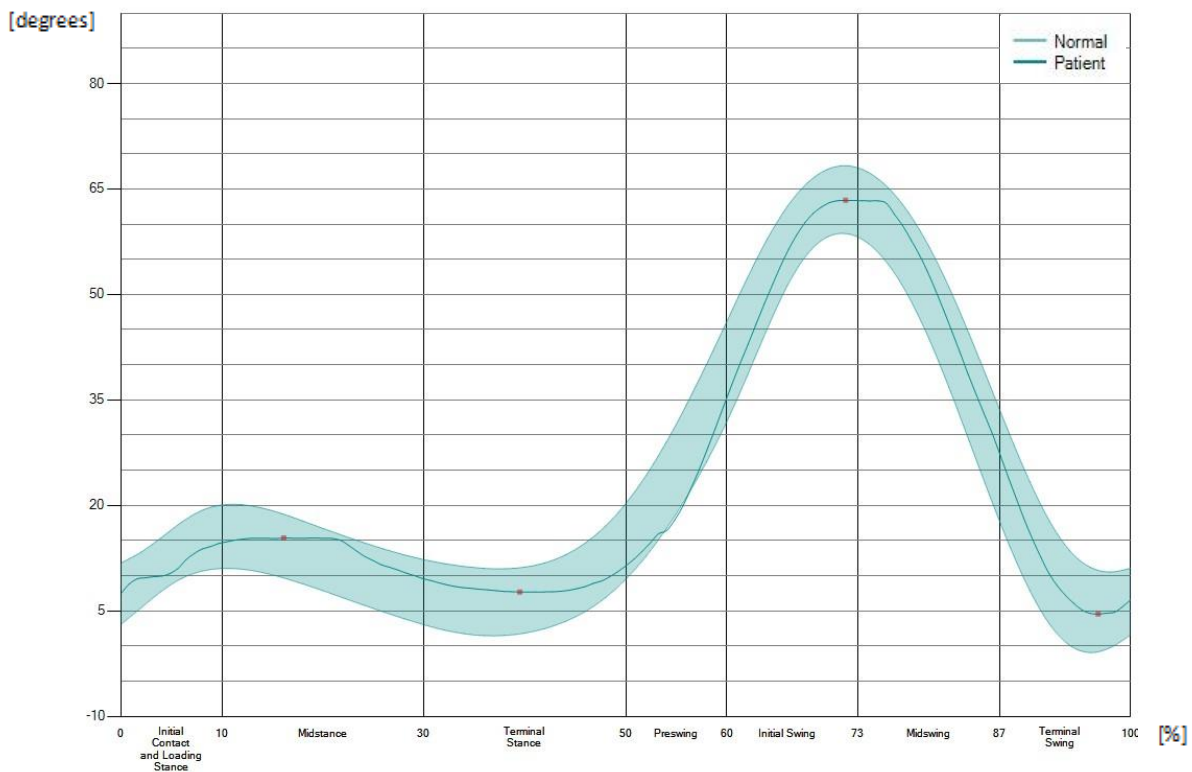


Figure 26: Encoder IKP best walking gait curve

Unlike the previous system, the IMU IKP did not show good results. As shown in Figure 27, the gait curve from the IMU IKP system has many disturbances, getting too far from the expected curve. This result may derive from the fusion between the accelerometer and gyroscope not being precise enough. In addition, the change of volumetry of the legs muscles while walking could affect the inclination of the IMUs, generating disruptions in the values.

After analysing and repeating the two systems' tests, the IMU IKP system still presented bad results. Due to that, we only proceeded to the following tests from these two systems with the Encoder IKP system. In order to verify if the Encoder IKP system is capable of getting good values in other situations, we did the subsequent tests:

- Compared the gait curves of 5 healthy volunteers in walk motion;
- Compared three different velocities gait curves of a healthy volunteer in walk motion;
- Compared three different walking time gait curves of a healthy volunteer;

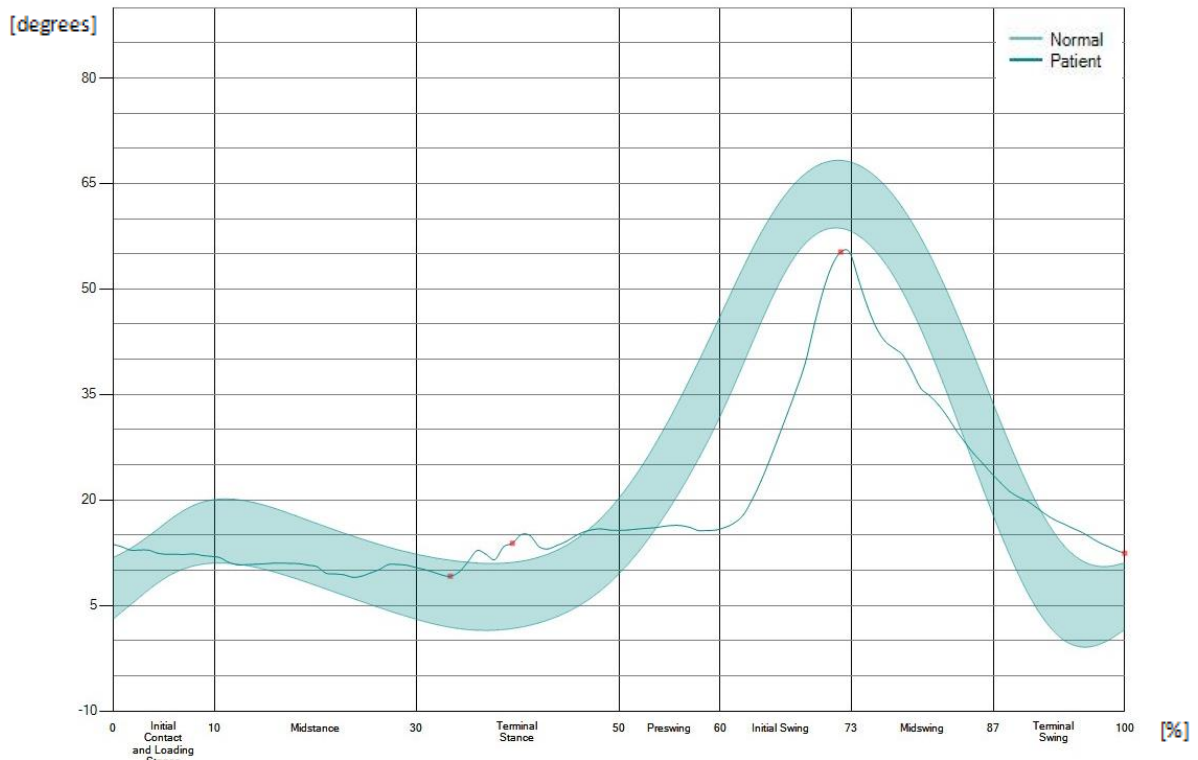


Figure 27: IMU IKP best walking gait curve

In this first experiment, all five volunteers were healthy men of 24 years old, with a mean high of 1,80 m. The experiment was conducted in environment A, and each volunteer has done a walking path of ten meters. From each volunteer test, was selected the best gait curve. These curves selection resulted in the chart of Figure 28.

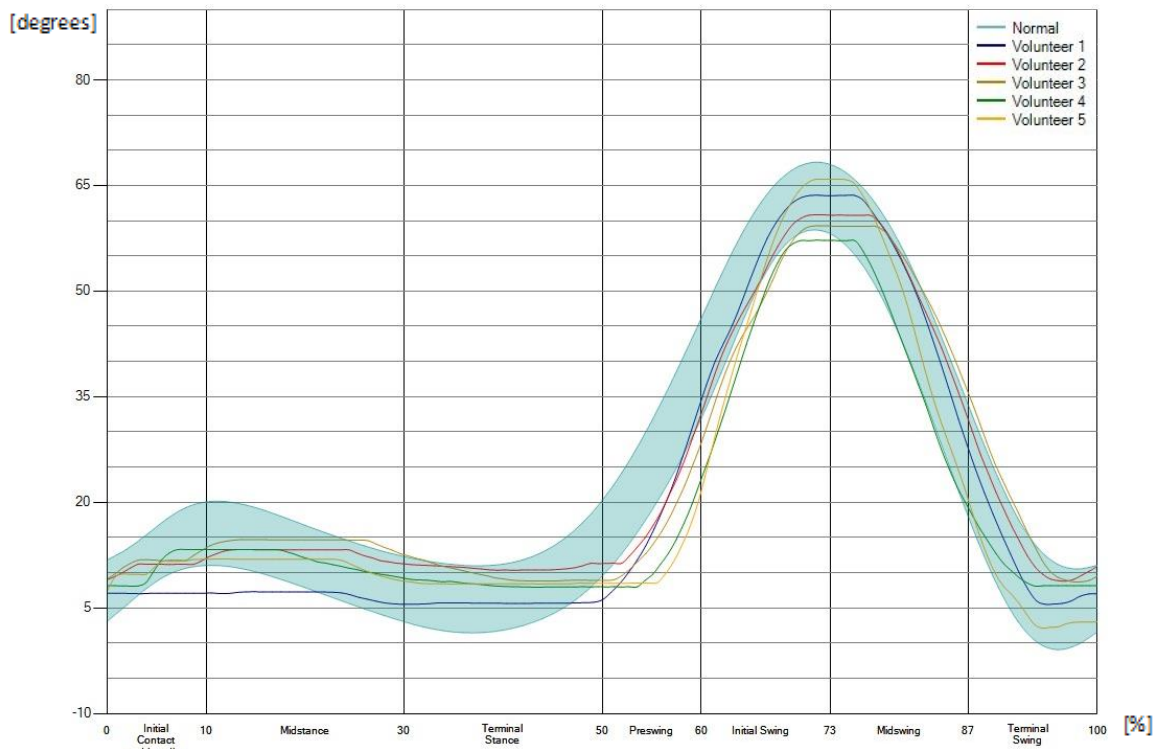


Figure 28: Encoder IKP gait curves from five healthy volunteers

Chapter 4. Tests and Results

The expected values for a normal gait curve have an average cadence of 80-100 steps/minute, and a Stance Phase representing 60% of the total gait and the Swing phase the remaining 40% [42]. From the tests with the five volunteers, were obtained the values represented in Table 4. These values and the curves obtained (Figure 28) show a great first confirmation of the encoder IKP to quantify a gait cycle. All Stance and Swing phases represent a mean of 60% and 40%, respectively, and almost every average cadence is between the expected interval, Table 4.

Table 4: Gait parameters from five healthy men

Volunteer	Maximum stance [degrees]	Minimum stance [degrees]	Maximum swing [degrees]	Minimum swing [degrees]	Stance time [s]	Swing time [s]	Average cadence [step/min.]
1	7	6	64	6	0.68	0.46	101.8
2	13	10	61	9	0.75	0.52	94.8
3	15	8	63	5	0.74	0.50	97.5
4	13	8	57	8	0.76	0.51	92.9
5	12	8	66	2	0.76	0.51	96.7

For a second experiment, were done some tests to compare multiple velocities. These tests were executed by a 54 years old healthy woman, 1.64 meters tall.

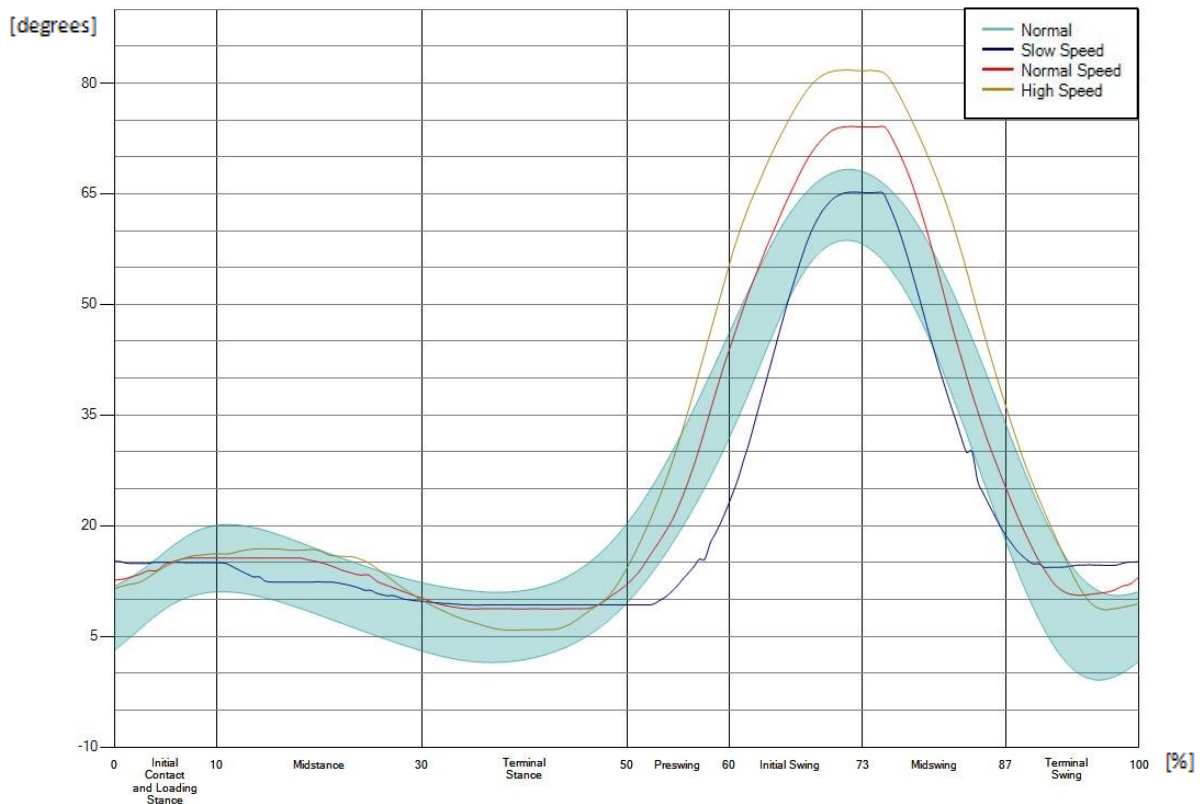


Figure 29: Encoder IKP different velocity gait curves from a healthy woman

It is expected from [42] that the slower the walking test is performed, the smaller the amplitudes, and the faster the walking test, the bigger the amplitudes. As expected, the amplitudes increase as fast as the walking test is performed, as shown in Figure 29. The values obtained from the velocity tests respect 60% for the Stance phase and 40% for the Swing phase, Table 5. On the other hand, the average cadence is slightly slower than 80 steps/minute but is predicted from [43], where it is described that the older the person, the slower is expected to walk.

Table 5: Gait parameters from a healthy woman – three different velocities

Volunteer speed	Maximum stance [degrees]	Minimum stance [degrees]	Maximum swing [degrees]	Minimum swing [degrees]	Stance time [s]	Swing time [s]	Average cadence [step/min.]
Slow	15	9	65	14	1.11	0.73	57.3
Normal	16	9	74	11	0.72	0.49	74.2
Fast	17	6	82	9	0.48	0.33	87.6

For the last experiment, were compared multiple tests with different time durations to verify any variations in the gait curve. These tests were executed by a healthy woman of 24 years old with 1.80 meters high. We have done three tests with different times duration: a 10 meters walking test, a 2 minutes test, and a 6 minutes test (like in [43]). To compare these tests was selected one gait curve from the middle of the total tests data. As shown in Figure 30, the results seem to be similar to each other. The maximum and minimum values from

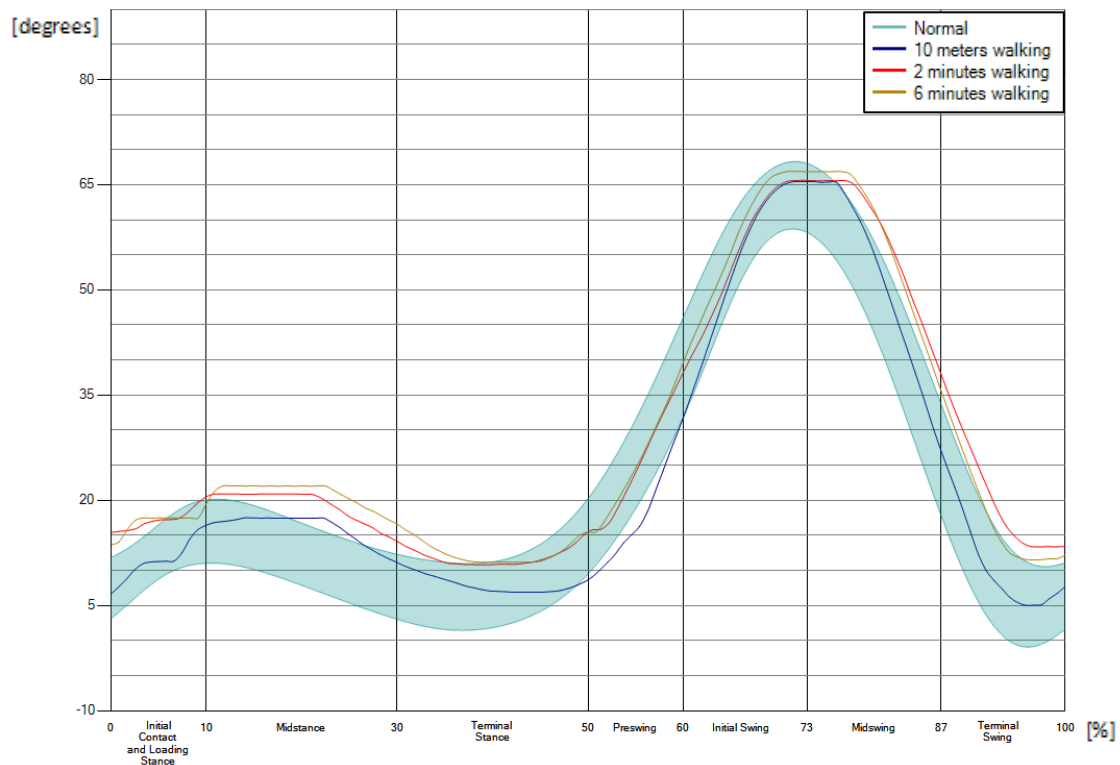


Figure 30: Encoder IKP gait curves from a healthy woman - different time duration tests

the three tests are close, and each test respects 60% for the Stance phase and 40% for the Swing phase (Table 6), proving that the Encoder IKP system measures are not affected by the test time scale.

Table 6: Gait parameters from a healthy woman – three different test duration

Volunteer test	Maximum stance [degrees]	Minimum stance [degrees]	Maximum swing [degrees]	Minimum swing [degrees]	Stance time [s]	Swing time [s]	Average cadence [step/min.]
10 meters walking	18	7	65	5	0.72	0.49	97.5.
2 minute walking	21	11	66	13	0.67	0.45	102.9
6 minute walking	22	11	67	12	0.72	0.48	109.4

After analysing the previous gaits from different tests, the gait curves of the two legs of one experience were analysed and compared between them. In Figure 31, it can be observed two gait curves, one from each leg of a healthy man of 24 years old with 1.82m high. In contrast, in Figure 32 it is presented two gait curves, one from each leg from a hurt man in the right knee, also 24 years old with 1,85m high. This injury resulted from a frontal collision with another man during sports practice, presenting swelling and bruising in the lateral region of the knee.

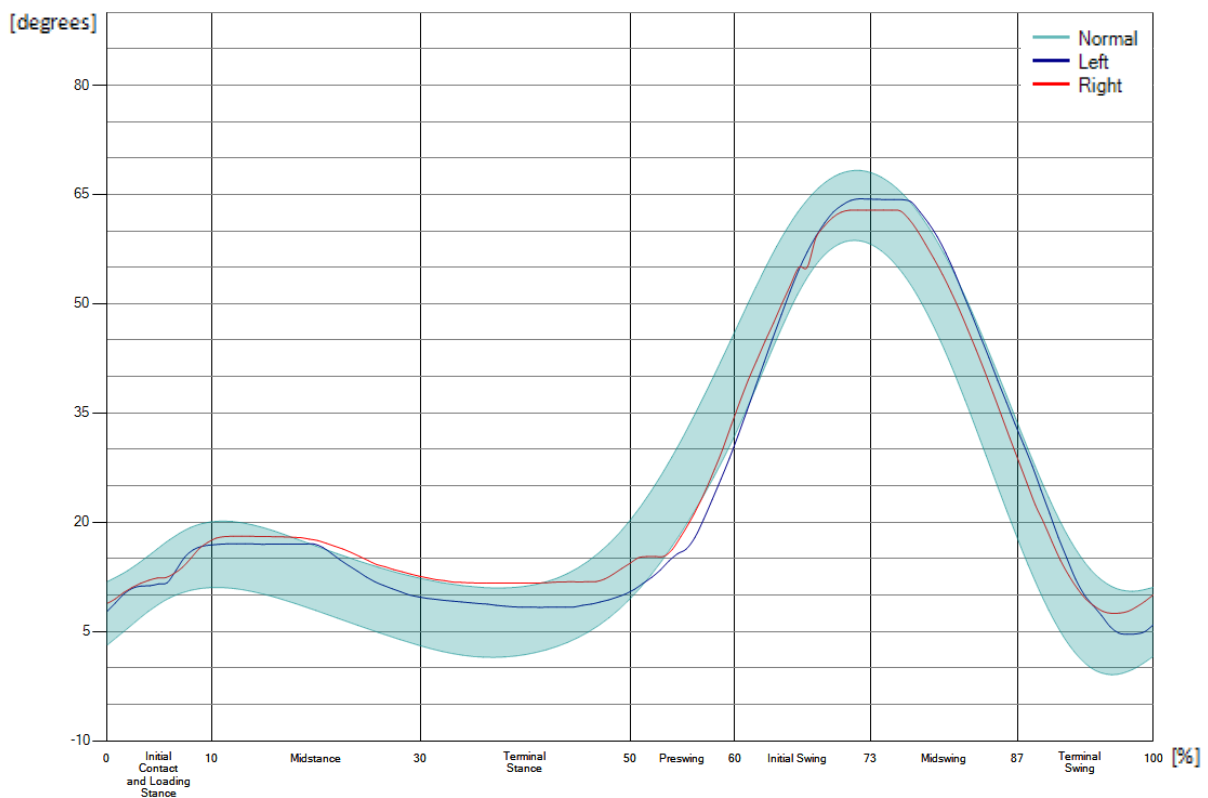


Figure 31: Encoder IKP gait curves for the two legs - healthy man

Table 7: Gait parameters from a healthy man – left and right legs

Volunteer knee	Maximum stance [degrees]	Minimum stance [degrees]	Maximum swing [degrees]	Minimum swing [degrees]	Stance time [s]	Swing time [s]
Left	17	8	64	5	0.72	0.49
Right	18	12	63	8	0.73	0.51

By comparing these two charts, it is easy to see that by observation, the Encoder IKP system is capable of detecting changes in the walking gait curve. In addition to the observation method, big differences can be detected by comparing the maximum and minimum values of Table 7 and Table 8.

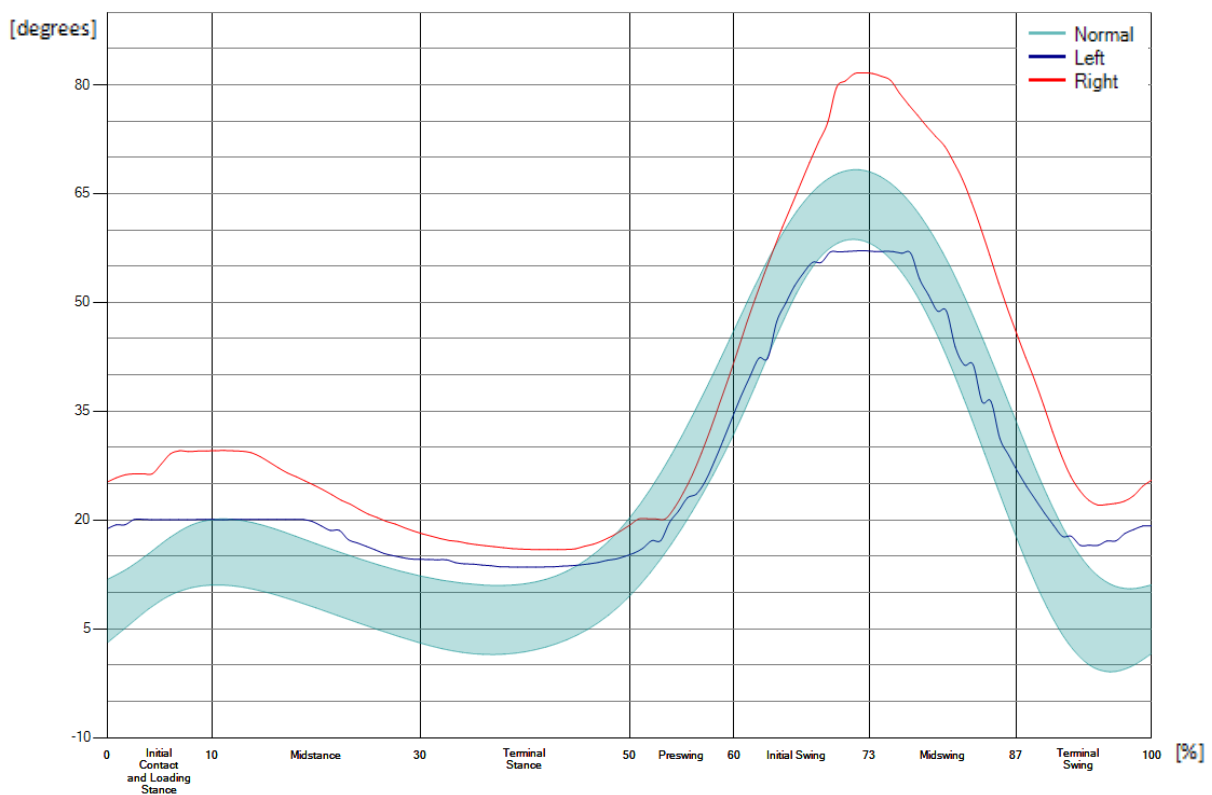


Figure 32: Encoder IKP gait curves for the two legs - hurt man

Table 8: Gait parameters from a hurt man – left and right legs

Volunteer knee	Maximum stance [degrees]	Minimum stance [degrees]	Maximum swing [degrees]	Minimum swing [degrees]	Stance time [s]	Swing time [s]
Left	20	14	57	17	0.70	0.46
Right	30	16	82	22	0.67	0.48

Additionally, the angular asymmetry shows a value of -6.00 to the healthy man and -17.45 to the hurt man. From Walter Herzog *et al.* [40], an asymmetry value starts defining an asymmetry when passed from 10. With this, we have another simple confirmation of the system results to describe the Knee Sagittal Plane Angle Curve and its perturbances.

With the Encoder IKP system and the developed application for this thesis, it is possible to measure and analyse more curves than the walking gait curves. We only analyse the walking gait curves in this work to prove that the system works for simple analysis. However, it is possible to measure a squat, to go upstairs and downstairs, as shown in Figure 33 and Figure 34.

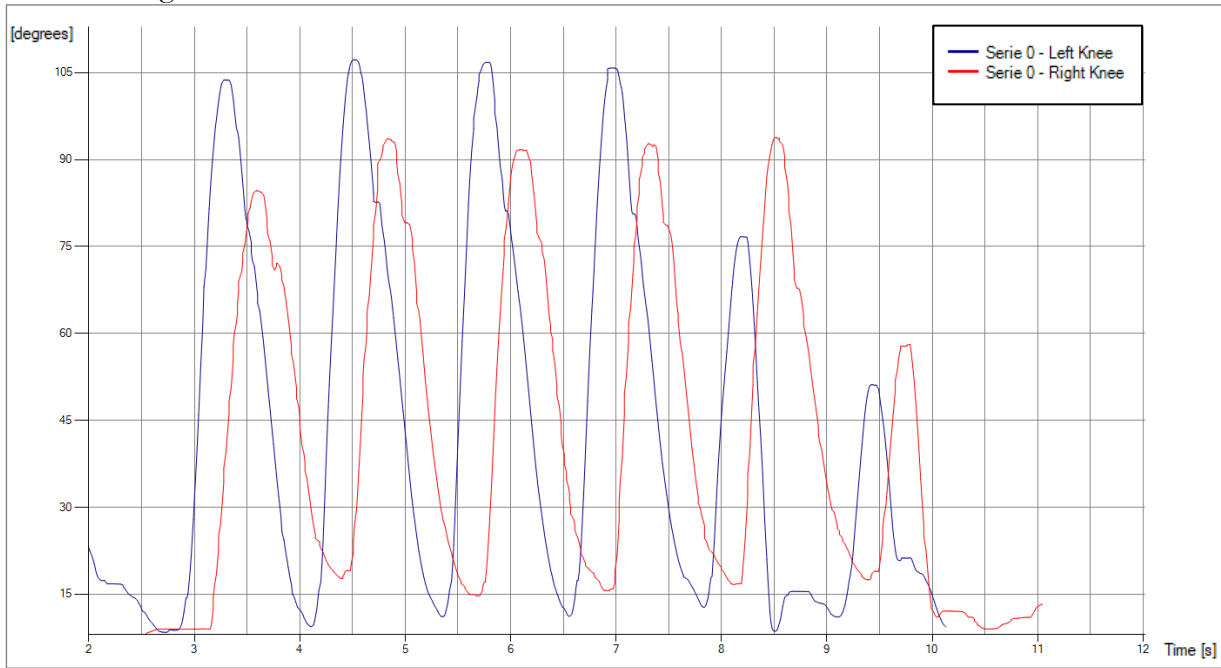


Figure 33: Knees sagittal joint angles trajectories when going upstairs

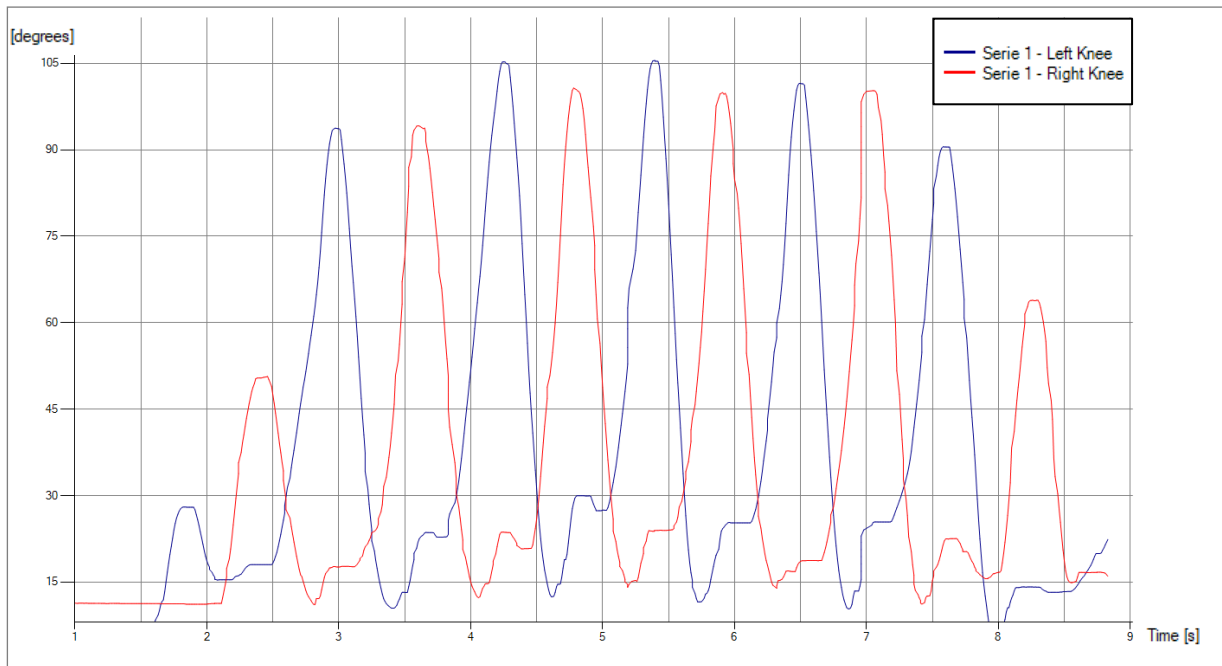


Figure 34: Knees sagittal joint angles trajectories when going downstairs

These curves have values that are pretty comparable to what may be predicted based on previous researches [44]. In the curve obtained climbing stairs, each step after reaching the maximum value, while decreasing, suffers a small peak, as expected. It is also observed that the dominant leg makes the values stand out in amplitude.

In the knee curve while going downstairs, the curve, while increasing, stabilizes for a short period before continuing to its maximum value. As descending stairs requires less effort from the legs, obtaining a synchronized step between the two knees is easier.

5. Conclusion and Future Work

5.1. Conclusion

This thesis set the goal to develop an entire low-cost wireless system, hardware and software, to measure and quantify the Knee Sagittal Plane Angle Curve (KSPAC). We have begun with two strategies to measure the KSPAC, with an IMU and with an Encoder.

At first, only the Encoder system was predicted for this work. However, the complexity of the hardware was not very high, due to the pandemic situation with the SARS-CoV-2 coronavirus, it was not easy to have all the material in the desired time, hindering the development of the work. Besides the difficulties arising from SARS-CoV-2, the Encoder model presented problems with a manufacturing defect, allowing only the device start-up with the MOSI channel physically disconnected. This problem delayed the development of the thesis even more. An answer from the supplier with the solution for the problem was only obtained three months after the contact. All these problems led to the development of work with the IMU system, adding the Encoder system to the work when the device problem was solved.

After the systems were developed and the feasibility had been checked, the first results with the IMU system did not show good values, essentially because the muscles' volumetry significantly affects the measurements. For this reason, we only proceeded with the Encoder Instrumented knee pad system to analyse the walking Knee Sagittal Plane Angle Curve.

Several tests were made to prove that the system could represent the Knee Sagittal Plane Angle Curve with the Encoder Instrumented knee pad system. These tests were done with several patients with the same characteristics in the same conditions. Speed tests and tests with different temporal values were also performed to reproduce different human gait conditions. In all these tests, the Encoder IKP system obtained very positive values in the representation of the KSPAC.

Adding to these tests, a comparison with the test of a person injured in the knee further reinforced the Encoder IKP system's viability for measuring human gait values and quantifying the test through the developed application.

In general, the work developed showed satisfactory results, where the main objective was, through a simple system, to be able to characterise the human gait at the knee level.

5.2. Future Work

Although the developed work already shows some progress in new strategies to analyse human gait, focusing on the sagittal plane of the knee, there are still improvements that can be added as future work.

As a first step towards the IMU Instrumented knee pad system, more precise IMUs can be used, including a magnetometer. In addition to a more accurate IMU, a more complex filter than the complementary filter can also be used, like the Kalman filter.

A different technique may be developed for the Instrumented knee pads system that gathers values for a mobile phone instead of a computer, making the system more mobile. Alternatively, a method that accumulates the values in the Instrumented knee pad until a Wi-Fi connection is re-established can be used.

It will also be interesting to compute and investigate the angular velocities and accelerations of the knee to have a more in-depth analysis of the knee sagittal plane angle using the developed IKP system. It is also important to create a technique that permits the identification of the offset that the leg has, with musculature, compared to the actual angle accomplished by the knee joint. This offset will allow eliminating the probable inaccuracies related to the leg's volumetry muscles.

6. References

- [1] V. T. I. H. D. E. J. B. dec. M. Saunders, "The Major Determinants in Normal and Pathological Gait," *Journal of Bone and Joint Surgery*, vol. 35, pp. 543-558, 1953.
- [2] W. Tao, T. Liu, R. Zheng and H. Feng, "Gait Analysis Using Wearable Sensors," *sensors*, 16 02 2012.
- [3] J. H. M. Fernandes, "Semiologia Ortopédica - Módulo 6, Marcha Humana," [Online]. Available: http://www.ufrgs.br/semiologiaortopedica/Modulo_6.pdf. [Accessed 04 julho 2020].
- [4] M. F. C. Molano, "ANÁLISIS Y DISEÑO DE CONTROLADORES NO LINEALES SOBRE UN SISTEMA ROBÓTICO BÍPEDO".
- [5] D. R. Labbe, N. Hagemester, M. Tremblay and J. d. Guise, "Reliability of a method for analyzing three-dimensional knee kinematics during gait," *Gait & Posture*, pp. 170-174, July 2008.
- [6] J. H. M. Fernandes, "Semiologia Ortopédica - Módulo 18, Joelhos e Pernas," [Online]. Available: http://www.ufrgs.br/semiologiaortopedica/Modulo_25.pdf. [Accessed 04 julho 2020].
- [7] A. G. N. Araújo, L. M. Andrade and R. M. L. d. Barros, "FISIOTERAPIA E PESQUISA,," *Sistema para análise cinemática da marcha humana baseado em videogrametria*, pp. 3-10, 2005.
- [8] J. Perry, "Gait Analysis," in *Normal and Pathological Function*, SLACK Incorporated, 1992, pp. 89-111; 223-245.
- [9] INCIBE, "incibe-cert," 03 05 2020. [Online]. Available: <https://www.incibe-cert.es/en/blog/ntp-sntp-and-ntp-what-time-synchronization-do-i-need>. [Accessed 30 05 2021].
- [10] Technologies, EndRun, "Introduction to NTP," p. 4.
- [11] T. Neagoe, V. Cristea and L. Banica, "NTP versus PTP in Computer Networks Clock," p. 6, 09 07 2006.
- [12] Orolia, "Differences Between NTP and SNTP," Orolia, 2019, p. 1.
- [13] P. Systems, "Perle Systems Technical Notes: PTP - Precision Time Protocol," Perle Systems, [Online]. Available: <https://www.perle.com/supportfiles/precision-time-protocol.shtml>. [Accessed 03 05 2021].

- [14] A. Muro-de-la-Herran, B. Garcia-Zapirain and A. Mendez-Zorrilla, "Gait Analysis Methods: An Overview of Wearable and Non-Wearable Systems, Highlighting Clinical Applications," p. 33, 19 02 2014.
- [15] A. N. M. Gomatam and S. Sasi, "MULTIMODAL GAIT RECOGNITION BASED ON STEREO VISION AND 3D TEMPLATE MATCHING," in *Proceedings of the International Conference on Imaging Science, Systems and Technology*, 2004.
- [16] H. Liu, Y. Cao and Z. Wang, "Automatic Gait Recognition From a Distance," in *Chinese Control and Decision Conference*, 2010.
- [17] A. Kolb, E. Barth, R. Koch and R. Larsen, "Time-of-Flight Sensors in Computer Graphics," EUROGRAPHICS, 2009.
- [18] D. Muramatsu, A. Shiraishi, Y. Makihara and Y. Yagi, "Arbitrary View Transformation Model for Gait Person Authentication," in *IEEE Fifth International Conference on Biometrics: Theory, Applications and Systems (BTAS)*, 2012.
- [19] M. O. Derawi, H. Ali and F. A. Cheikh, "Gait Recognition using Time-of-Flight Sensor".
- [20] S. S. Inc., SurvTech Solutions Inc., [Online]. Available: <https://www.survtechsolutions.com/how-does-laser-scanning-work>. [Accessed 28 05 2021].
- [21] T. Pallejà, M. Teixidó, M. Tresanchez and J. Palacín, "Measuring Gait Using a Ground Laser Range Sensor," *Sensors*, 2009.
- [22] M. F. Abadía, M. Sillero-Quintana and P. Á. M. Calvo, "Applying Topographic Techniques to Modeling the Human Shape in Motion," in *Second Workshop on Digital Media and its Application in Museum*, 2007, pp. 169-172.
- [23] A. H. A. Razak, A. H. A. Razak, R. K. Begg and Y. Wahab, "Foot Plantar Pressure Measurement System: A Review," p. 30, 23 07 2012.
- [24] C. V. C. Bouten, K. T. M. Koekkoek, M. Verduin, R. Kodde and J. D. Janssen, "A Triaxial Accelerometer and Portable Data Processing Unit for the Assessment of Daily Physical Activity," *IEEE TRANSACTIONS ON BIOMEDICAL ENGINEERING*.
- [25] H. Zeng and Y. Zhao, "Sensing Movement: Microsensors for Body Motion Measurement," *sensors*, p. 638–660, 2011.
- [26] P. Catalfamo, S. Ghoussayni and D. Ewins, "Gait Event Detection on Level Ground and Incline Walking Using a Rate Gyroscope," *sensors*, 2010.
- [27] O. Tunçel, K. Altun and B. Barshan, "Classifying Human Leg Motions with Uniaxial Piezoelectric Gyroscopes," *sensors*, 2009.
- [28] K. J. O'Donovan, R. Kamnik, D. T. O'Keefe and G. M. Lyons, "An inertial and magnetic sensor based technique for joint angle measurement," *Jornal of Biomechanics*, 2007.

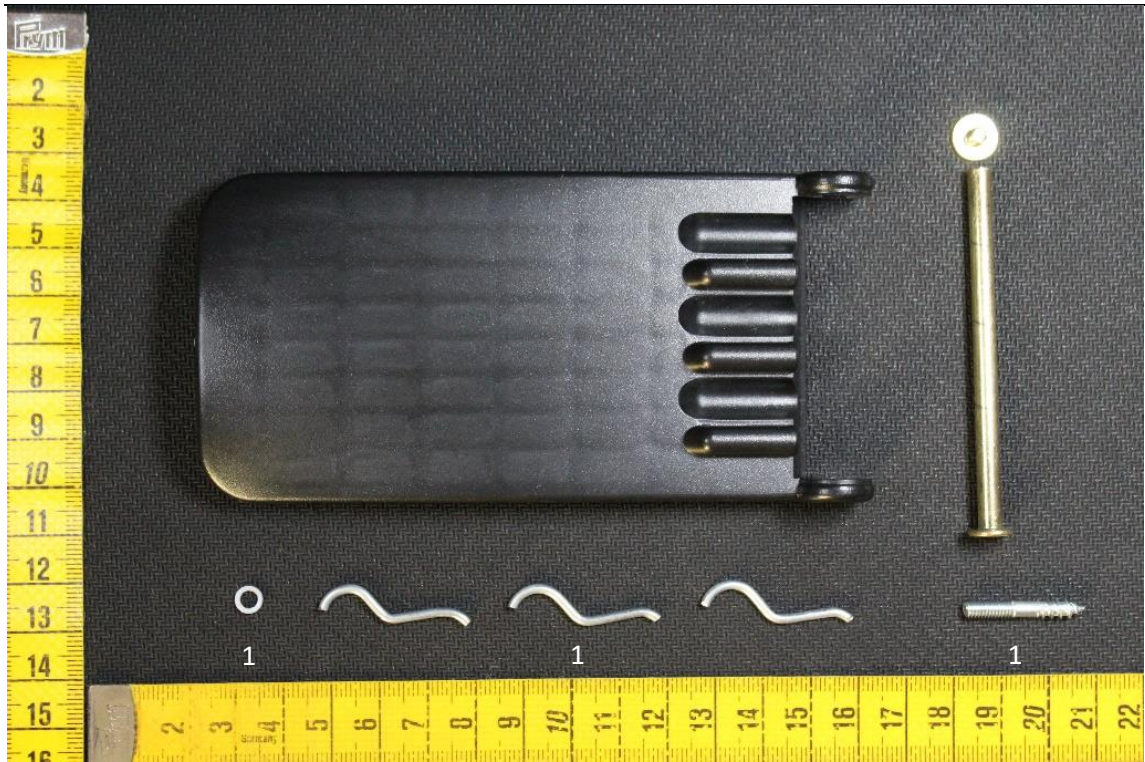
- [29] P. Piriyaarasarth, M. E. Morris, A. Winter and A. E. Bialocerkowski, "The reliability of knee joint position testing using electrogoniometry," *BioMed Central*, 2008.
- [30] R. Roduit, P.-A. Besse and a. J.-P. Micallef, "Flexible Angular Sensor," in *IEEE Transactions on Instrumentation and Measurement*.
- [31] "Electro-goniometric system: An instrumentation to capture knee movements for forward walking," in *10th Asian Control Conference (ASCC)*, 2015.
- [32] A. D. Milne, D. G. Chess, J. A. Johnson and G. j. W. King, "Accuracy of an electromagnetic tracking device: A study of the optimal operating range and metal interference," *Journal of Biomechanics*, p. 791–793, 1996.
- [33] A. M. J. Bull, F. H. Berkshire and A. A. Amis, "Accuracy of an electromagnetic measurement device and application to the measurement and description of knee joint motion.," *Journal of Engineering in Medicine*, p. 347–355, 1998.
- [34] P. M. Mills, S. Morrison, D. G. Lloyd and R. S. Barrett, "Repeatability of 3D gait kinematics obtained from an electromagnetic tracking system during treadmill locomotion.," *Journal of Biomechanics*, p. 1504–1511, 2007.
- [35] Dynapar, Encoder Communications Handbook, Dynapar, Gurne , IL, 2007.
- [36] CUI, "CUI Devices," [Online]. Available: <https://www.cuidevices.com/product/motion/rotary-encoders/absolute/modular/amt22-series>. [Accessed 24 05 2020].
- [37] C. Devices, "AMT22 Arduino SPI Sample Code Tutorial," CUI Devices, [Online]. Available: <https://www.cuidevices.com/product/resource/sample-code/amt22>. [Accessed 2020 12 20].
- [38] C. J. Fisher, "Using an Accelerometer for Inclination Sensing," Analog Devices, [Online]. Available: <https://www.analog.com/en/app-notes/an-1057.html>. [Accessed 2020 11 27].
- [39] R. S. Gonçalves, J. Cabri and J. P. Pinheiro, "Cross-cultural adaptation and validation of the Portuguese version of the Knee Outcome Survey-Activities of Daily Living Scale (KOS-ADLS)," p. 5, 5 Setembro 2008.
- [40] W. Herzog, B. M.Nigg, L. J. Read and E. Olsson, "Asymmetris in ground reaction force patterns in normal human gait," 1989.
- [41] N. Darras, M. Tziomaki and D. Pasparakis, "Gait Analysis ADplot," 23 05 2020. [Online]. Available: <https://sites.google.com/site/gaitanalysisadplot/basic-elements/gait-graph-deviation-index?authuser=0>. [Accessed 18 10 2021].
- [42] H. Uustal, "Normal Gait," Prosthetic/Orthotic Team JFK-Johnson Rehab Institute.
- [43] Physiopedia, "10 Metre Walk Test," Physiopedia, [Online]. Available: https://www.physio-pedia.com/10_Metre_Walk_Test. [Accessed 2021 7 19].

- [44] S.-E. Park, Y.-J. Ho, M. H. Chun, J. Choi and Y. Moon, "Measurement and Analysis of Gait Pattern during Stair Walk for," *Hindawi*, vol. 2019, p. 12, 3 10 2019.
- [45] K. McQuade, J. SIDLES and R. LARSON, "Reliability of the Genucom Knee Analysis System," *Clinical orthopaedics and related research*, 1989.
- [46] I. Susnea and M. Mitescu, *Microcontrollers in Practice*, Springer, 2005.
- [47] S. d. Oliveira, *Internet das Coisas com ESP8266, Arduino e Raspberry Pi*, Novatec Editora, 2017.
- [48] "ESPRESSIF," [Online]. Available: <https://www.espressif.com/en/products/socs/esp8266/overview>. [Accessed 28 junho 2020].
- [49] H. S. Mendonça. [Online]. Available: <https://paginas.fe.up.pt/~hsm/docencia/comp/spi-e-i2c/>. [Accessed 01 julho 2020].
- [50] Arduino, "SPI library," [Online]. Available: <https://www.arduino.cc/en/reference/SPI>. [Accessed 01 julho 2020].
- [51] E. Systems, "ESP-IDF Programming Guide," [Online]. Available: <https://docs.espressif.com/projects/esp-idf/en/latest/esp32/api-guides/mesh.html>. [Accessed 01 julho 2020].
- [52] E. I. Team, *ESP8266 Mesh User Guide*, Espressif Inc..
- [53] F. J. F.-P. R. J. V.-S. J. M.-P. J. M. G.-C. Mario Nieto-Hidalgo, "A vision based proposal for classification of normal and abnormal gait using RGB camera," p. 8, 4 agosto 2016.

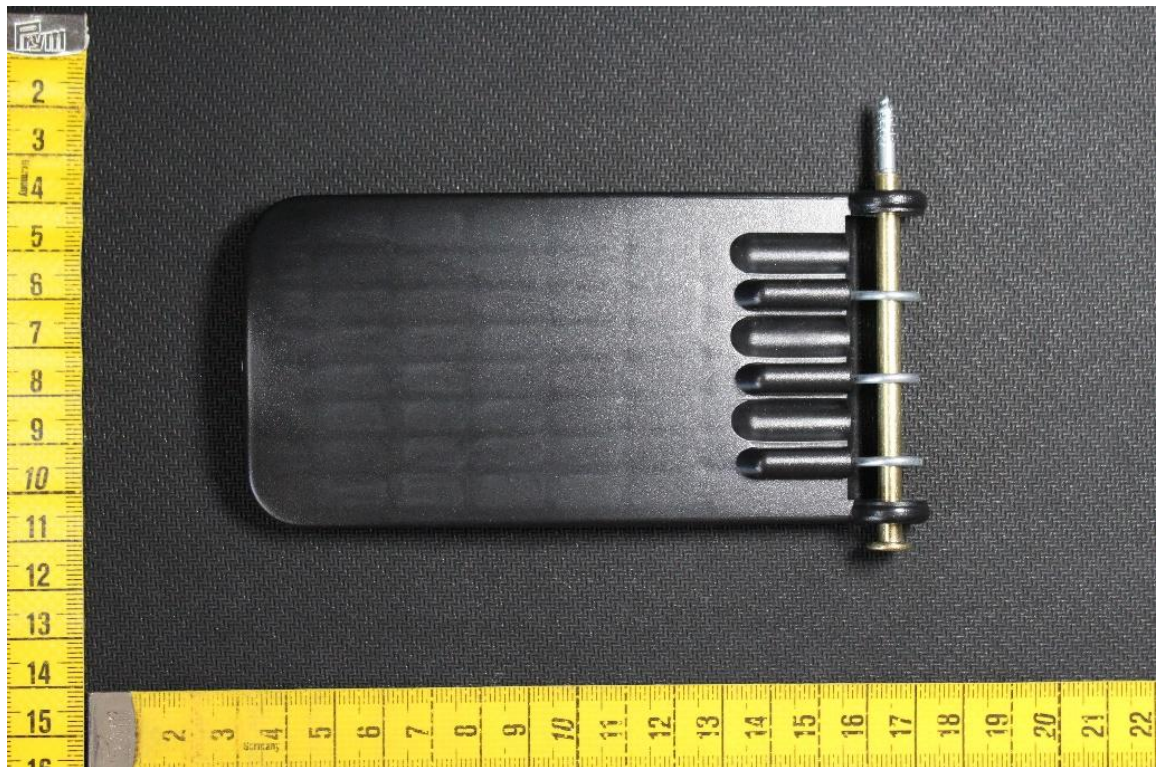
APPENDIX A

SYSTEMS ASSEMBLY

APPENDIX - A

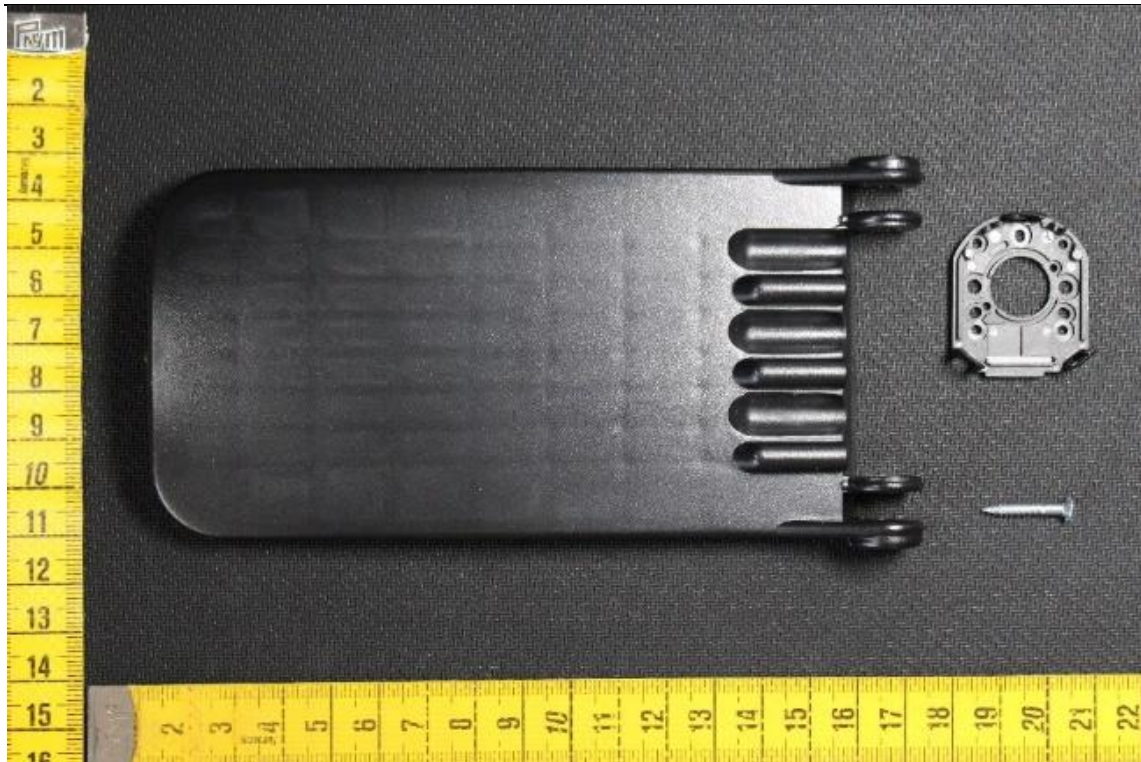


Calf Rigid Plastic Structure unmounted

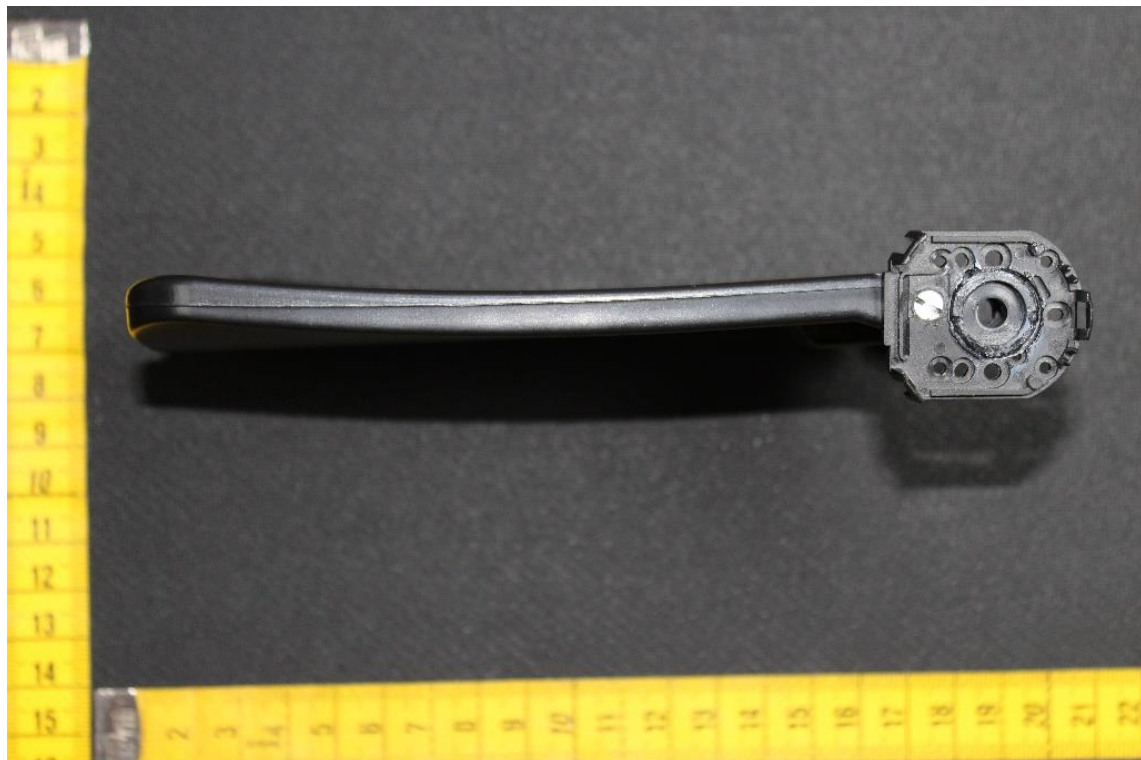


Calf Rigid Plastic Structure mounted

APPENDIX - A



Thigh Rigid Plastic Structure unmounted

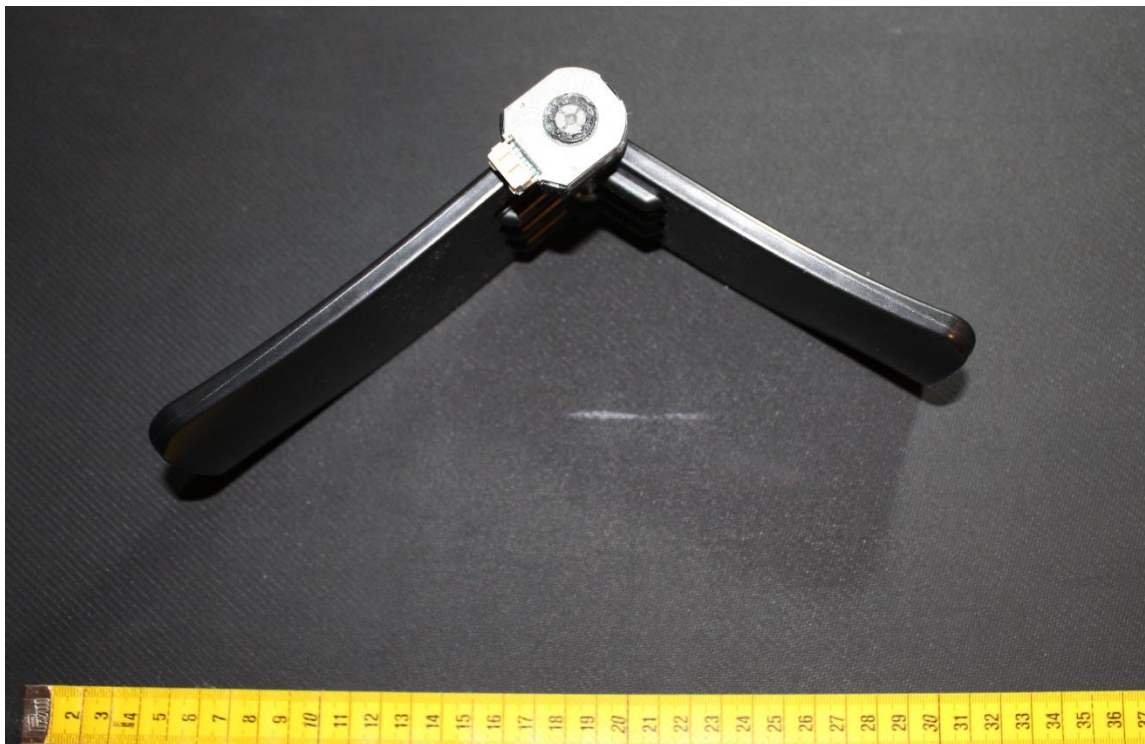


Thigh Rigid Plastic Structure mounted

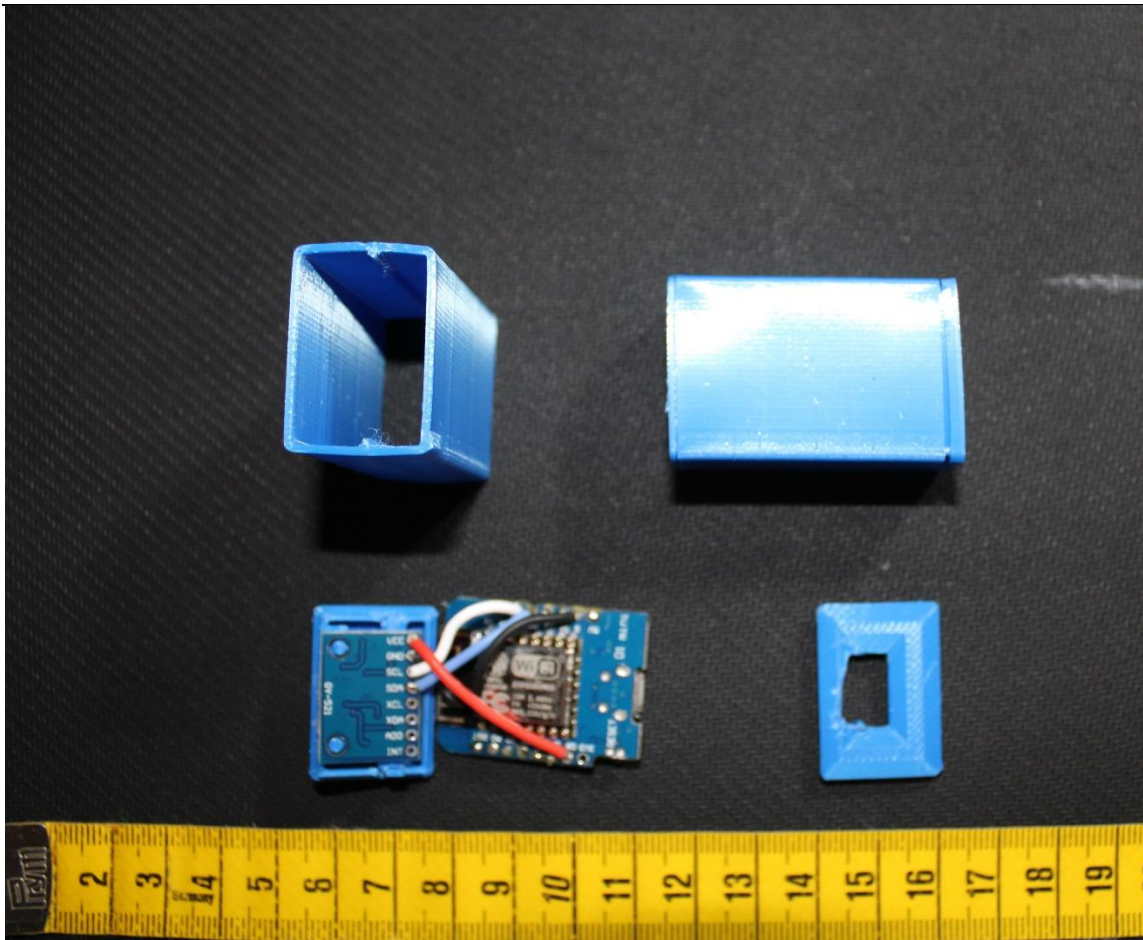
APPENDIX - A



Encoder IKP mounted structure



Complete Encoder IKP



IMU IKP case and hardware (IMU + Wemos D1 mini)

APPENDIX B

CODE SCRIPTS

Encoder IKP functions from the crated library to read the values from the encoder. Code in C++

```

/* AMT22_SPI.cpp - Library for flashing AMT22 SPI connection.
 * Created by Miguel L. Rodrigues, January 9, 2021.
 * Released into the public domain. */

#include "AMT22_SPI.h"

/* SPI commands */
#define AMT22_NOP      0x00
#define AMT22_RESET   0x60
#define AMT22_ZERO     0x70

/* We will use these define macros so we can write code once compatible with 12 or 14 bit
encoders */
#define RES12          12
#define RES14          14

/*This function gets the absolute position from the AMT22 encoder using the SPI bus. The AMT22
position includes 2 checkbits to use
 * for position verification. Both 12-bit and 14-bit encoders transfer position via two bytes,
giving 16-bits regardless of resolution.
 * For 12-bit encoders the position is left-shifted two bits, leaving the right two bits as
zeros. This gives the impression that the encoder
 * is actually sending 14-bits, when it is actually sending 12-bit values, where every number is
multiplied by 4.
 * This function takes the pin number of the desired device as an input
 * This function expects res12 or res14 to properly format position responses.
 * Error values are returned as 0xFFFF */

uint16_t getPositionSPI(uint8_t encoder, uint8_t resolution)
{
    uint16_t currentPosition;           //16-bit response from encoder
    bool binaryArray[16];              //after receiving the position we will populate this array and
                                        use it for calculating the checksum

    //get first byte which is the high byte, shift it 8 bits. don't release line for the first byte
    currentPosition = spiWriteRead(AMT22_NOP, encoder, false) << 8;

    //This is the time required between bytes as specified in the datasheet. (recommended 3us)
    //We will implement that time delay here; however, the Arduino is not the fastest device, so the
    delay is likely inherently there already
    delayMicroseconds(4); //meter a 4us MR [07_01_2021]

    //OR the low byte with the currentPosition variable. release line after second byte
    currentPosition |= spiWriteRead(AMT22_NOP, encoder, true);

    //run through the 16 bits of position and put each bit into a slot in the array so we can do
    the checksum calculation
    for(int i = 0; i < 16; i++) binaryArray[i] = (0x01) & (currentPosition >> (i));

    //using the equation on the datasheet we can calculate the checksums and then make sure they
    match what the encoder sent
    if ((binaryArray[15] == !(binaryArray[13] ^ binaryArray[11] ^ binaryArray[9] ^ binaryArray[7]
^ binaryArray[5] ^ binaryArray[3] ^ binaryArray[1]))
        && (binaryArray[14] == !(binaryArray[12] ^ binaryArray[10] ^ binaryArray[8] ^
binaryArray[6] ^ binaryArray[4] ^ binaryArray[2] ^ binaryArray[0])))
    {
        //we got back a good position, so just mask away the checkbits
        currentPosition &= 0x3FFF;
    }
    else
    {
        currentPosition = 0xFFFF; //bad position
    }

    //If the resolution is 12-bits, and wasn't 0xFFFF, then shift position, otherwise do nothing
    if ((resolution == RES12) && (currentPosition != 0xFFFF)) currentPosition = currentPosition >>
2;

    return currentPosition;
}

```


Matlab function which calculates the parameters of the gait curve to compare with the normal gait curve.

```
function [timeTo_HundredPerCent, angles, times, HowManyGaits, max_Swing,
max_Stance, min_Swing, min_Stance, percentageIN] = GaitCurveVSNormal(angule_in, time_in, Gait)
    P=0.5;
    [~, A_val] = islocalmax(angule_in, 'MinProminence', P); % get the maximum values from gait measure

    % Normal gait values - Knee Sagital Angles
    SagitalKneeAngles = [3.08393884 5.423778515 7.779109913 9.611110936
10.65998851 11.04285775 10.9343333 10.46752232 9.746130542 8.860006132
7.879479969 6.861502172 5.844945908 4.853016318 3.905374955 3.031144039
2.287242096 1.750184748 1.481313498 1.509302333 1.841731908 2.490456445
3.493144864 4.925047066 6.887954641 9.477756188 12.74839313 16.66206249
21.14575426 26.1890383 31.90156136 38.33406106 45.09653232 51.25238673
55.7849152 58.21351745 58.62657528 57.2606416 54.25913034 49.71232549
43.78630054 36.79542733 29.19905102 21.51743608 14.25383896 7.916897026
3.035142261 0.047851452 -0.926605234 -0.213690152 1.592153808];
    SagitalKneeAnglesAvg = [11.81907289 13.35853478 15.4105759
17.61505787 19.28698615 20.08102339 20.11796746 19.63397855 18.81223592
17.8019105 16.73860159 15.7079222 14.73211741 13.81687377 12.9913707
12.29007505 11.72603334 11.30635108 11.05036242 10.99956844 11.22952298
11.84344343 12.95651027 14.67544093 17.08921612 20.26928176 24.25120948
28.97066358 34.30077203 40.08781159 46.16517176 52.25191021 57.87619874
62.5339613 65.89084773 67.81497477 68.29652146 67.39368486 65.16430941
61.64203806 56.89150745 51.05741642 44.40827208 37.30175566 30.14258189
23.40715647 17.67902857 13.52259379 11.20117599 10.54092593
11.075107340];

    t = 0:2:100;
    [~,q] = max(SagitalKneeAnglesAvg);
    NormalMax_t = t(q)/100; % localise the percente in a gate cycle
of the Maximum angule in Normal Measure

    T_up = find(A_val>20); % get the maximum values under 20
    [~, sizeT_up] = size(T_up);

    % removing the maximums closed values
    T_up_aux = logical(ones(1, sizeT_up)); %#ok<*LOGL>
    for j = 1:sizeT_up
        if(j<sizeT_up)
            if( (T_up(j+1))>=(T_up(j)-4)) && (T_up(j+1)<=(T_up(j)+4)) )
                T_up_aux(j+1) = false;
            end
        end
    end

    % calcule of gait maximum values indexes
    GaitMaxIndexs = T_up(T_up_aux);
    % calcule of period indexes
    Period_in_Index = GaitMaxIndexs(Gait) - GaitMaxIndexs(Gait-1);
    % calcule of maximum normal gait value index
    IndexsTo_MaxGaitIndex = round(Period_in_Index*NormalMax_t);
    [~, HowManyGaits] = size(GaitMaxIndexs);

    beforeMax = IndexsTo_MaxGaitIndex;
```

```

afterMax = Period_in_Index - beforeMax;

if Gait==1
    angles = angle_in(1:(GaitMaxIndexs(Gait)+afterMax));
    times = time_in(1:(GaitMaxIndexs(Gait)+afterMax));
elseif Gait == HowManyGaits
    angles = angle_in((GaitMaxIndexs(Gait)-beforeMax):end);
    times = time_in((GaitMaxIndexs(Gait)-beforeMax):end);
else
    angles = angle_in((GaitMaxIndexs(Gait)-beforeMax):(GaitMax-
Indexs(Gait)+afterMax));
    times = time_in((GaitMaxIndexs(Gait)-beforeMax):(GaitMax-
Indexs(Gait)+afterMax));
end

[~, s] = size(angles);
timeTo_HundredPerCent = 0:100/(s-1):100;

angles_max_Swing = angles(round(s*0.5):s);
angles_min_Swing = angles(round(s*0.73):s);
angles_max_Stance = angles(round(s*0.1):round(s*0.4));
angles_min_Stance = angles(round(s*0.3):round(s*0.6));

time_max_Swing = timeTo_HundredPerCent(round(s*0.5):s);
time_min_Swing = timeTo_HundredPerCent(round(s*0.73):s);
time_max_Stance = timeTo_HundredPerCent(round(s*0.1):round(s*0.4));
time_min_Stance = timeTo_HundredPerCent(round(s*0.3):round(s*0.6));

[Value_max_Swing, Index_max_Swing] = max(angles_max_Swing);
[Value_min_Swing, Index_min_Swing] = min(angles_min_Swing);
[Value_max_Stance, Index_max_Stance] = max(angles_max_Stance);
[Value_min_Stance, Index_min_Stance] = min(angles_min_Stance);

max_Swing = [Value_max_Swing, time_max_Swing(Index_max_Swing)];
min_Swing = [Value_min_Swing, time_min_Swing(Index_min_Swing)];
max_Stance = [Value_max_Stance, time_max_Stance(Index_max_Stance)];
min_Stance = [Value_min_Stance, time_min_Stance(Index_min_Stance)];

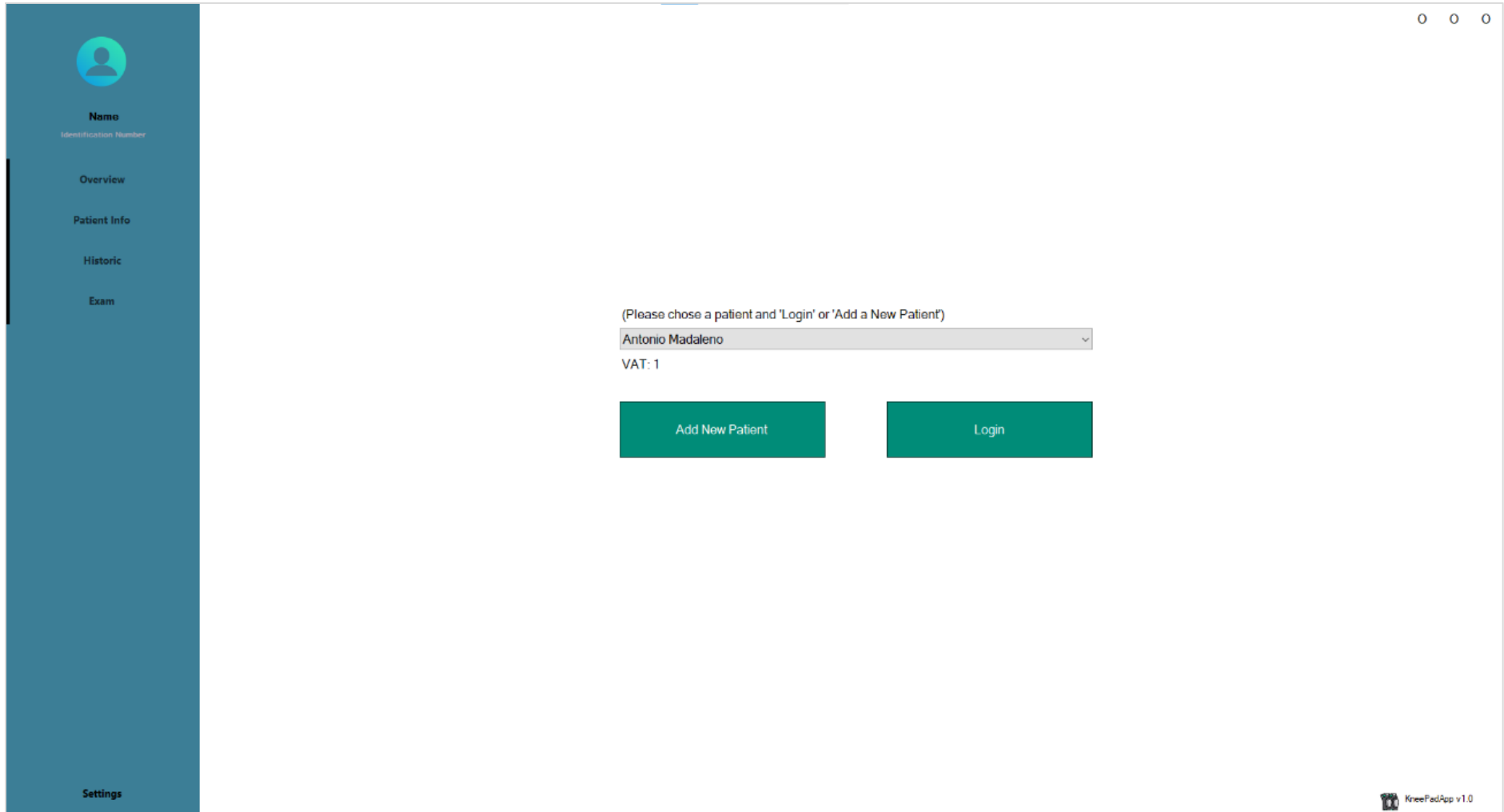
% calculc of gait % inside normal gait
SagitalKneeAnglesArea = polyshape([t fliplr(t)]), {[SagitalK-
neeAngles fliplr(SagitalKneeAnglesAvg)]});
TFin = isinterior(SagitalKneeAnglesArea, timeTo_HundredPerCent, an-
gles);
percentageIN = sum(TFin)/size(TFin,1)*100;

end

```

APPENDIX C

APPLICATION FEATURES



Application Main Page

*REQUIRED

IDENTITY NUMBER	7
NAME	
SEX	
BIRTH DATE	01/01/1920
WEIGHT	0,0 kg
HIGHT	0 cm
VAT NUMBER	
MOBILE NUMBER	
ADRESS	
FIRST REGISTRATION	06/07/2021
DOMINANT LEG	

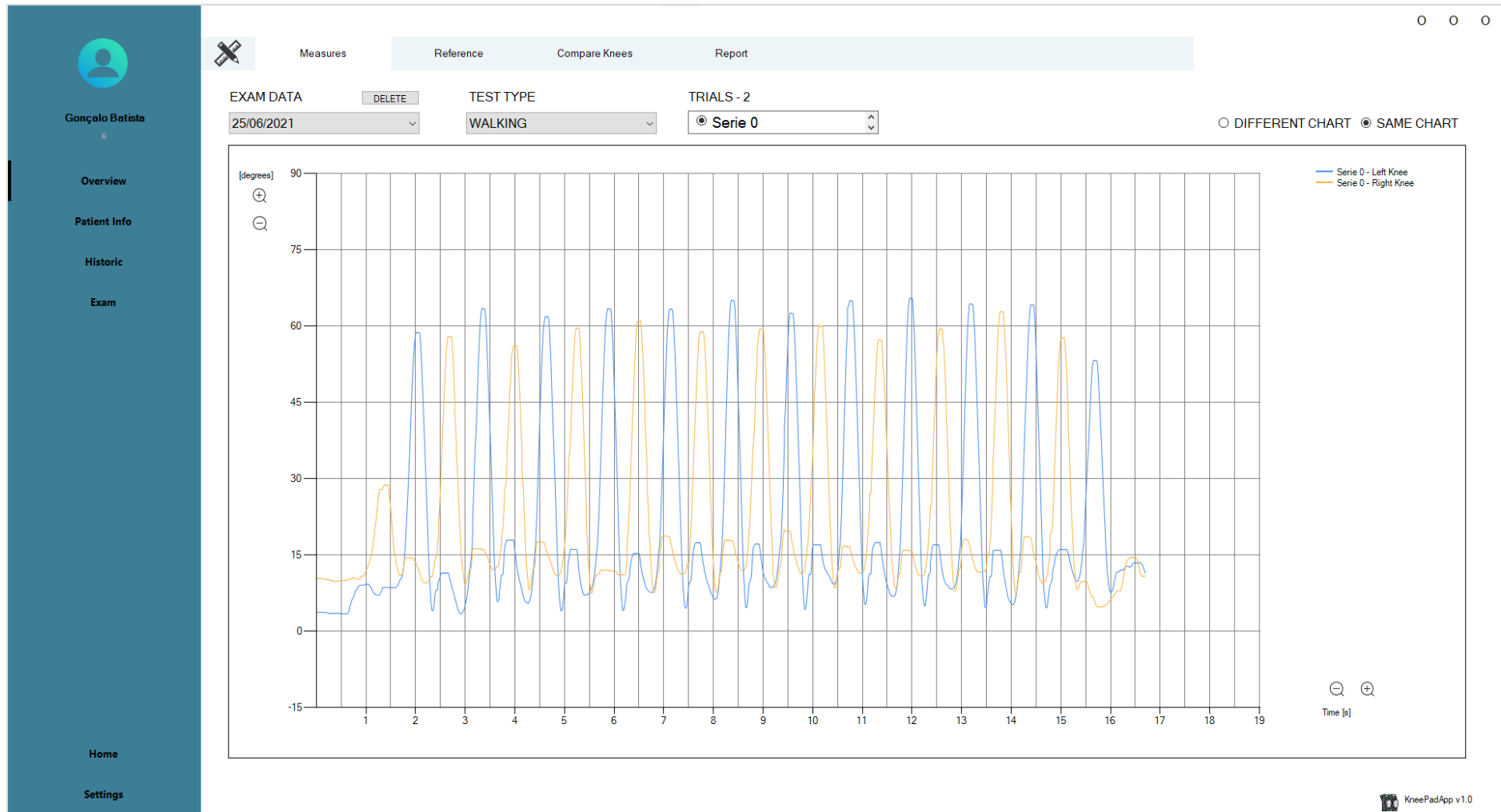
OBSERVATIONS

SUBMIT

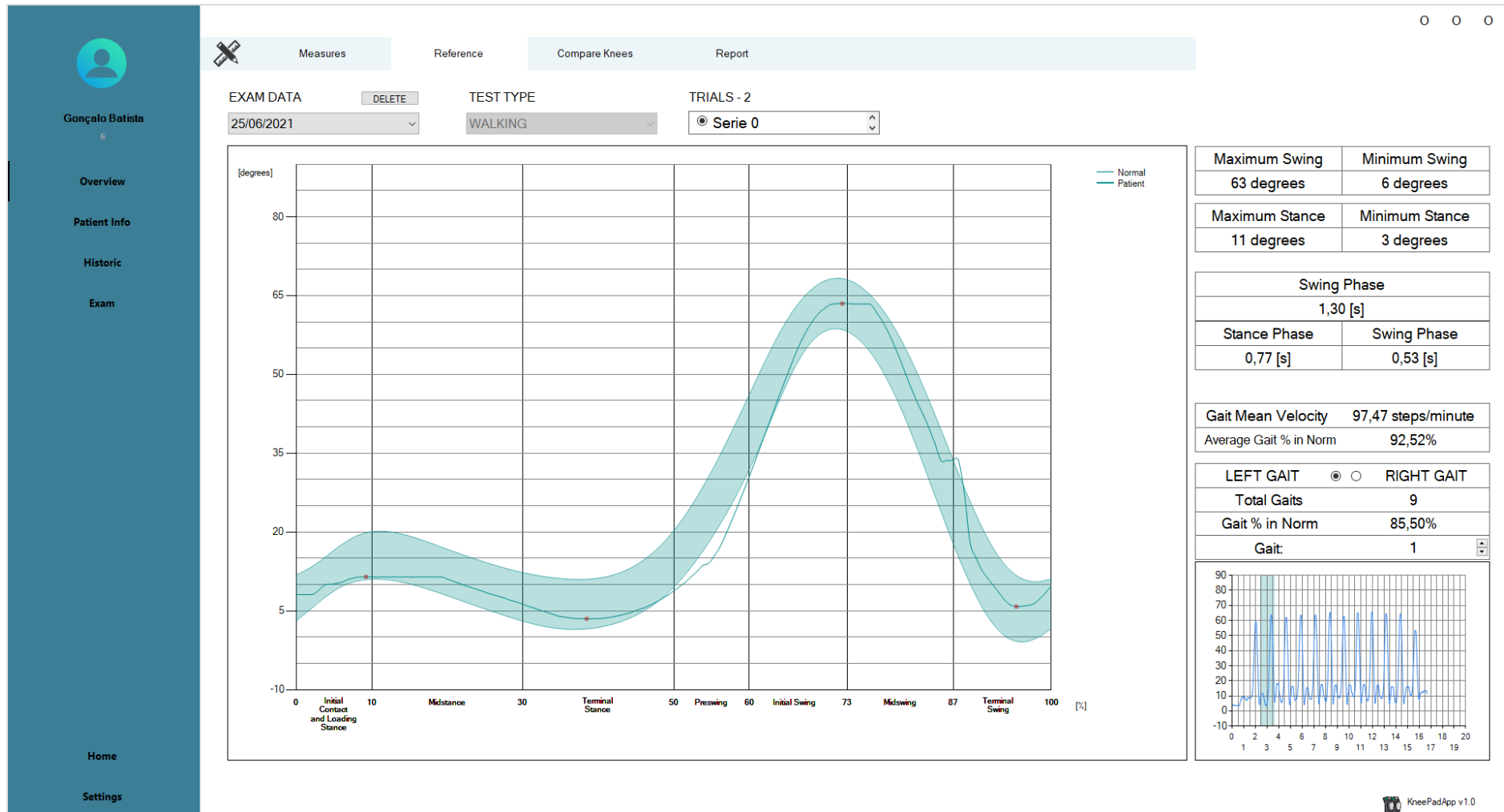
Home
Settings

KneePadApp v1.0

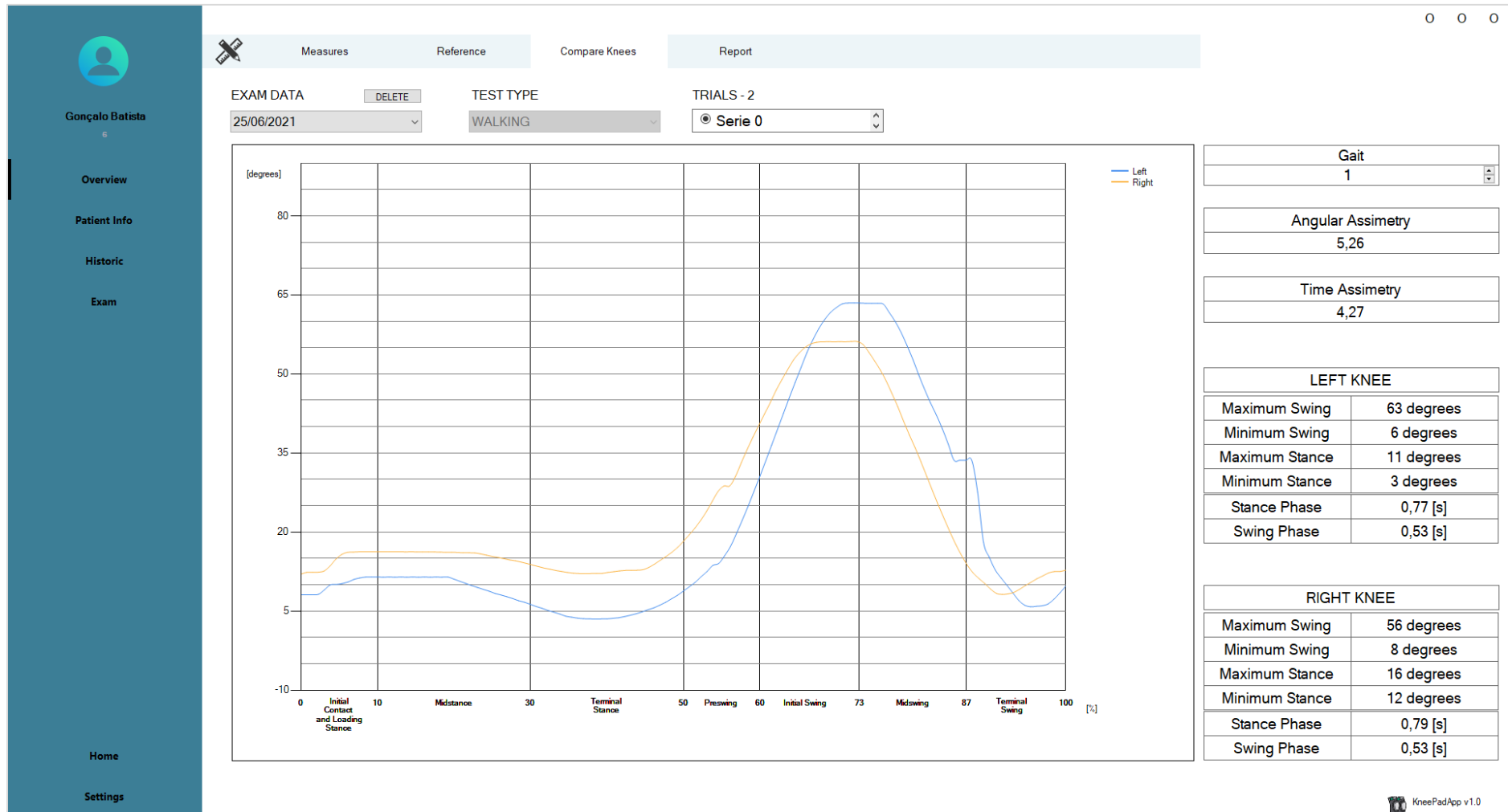
New patient page > Where to insert the personal information from the patient.



Overview Page > Measures subpage, where it is shown all the gait curves from a test.



Overview Page > Reference subpage, where it is shown each gait details from a test and it is compared with the norm gait curve.




Overview Page > Compare Knees subpage, where it is presented each knee gait curve parameters and the angular and time asymmetries values.

IDENTITY NUMBER	4
NAME	Martin Estominho
SEX	MALE
BIRTH DATE	01/07/1998
WEIGHT	0,0 kg
HIGHT	0 cm
VAT NUMBER	66666
MOBILE NUMBER	0
ADDRESS	
FIRST REGISTRATION	24/06/2021
DOMINANT LEG	RIGHT
OBSERVATIONS	

EDIT

KneePadApp v1.0

Patient Info Page > Where to consult and edit the personal information from the patient.



Antonio Madaleno

2

Overview

Patient Info

Historic

Exam

Home

Settings

fevereiro de 2021						
dom	seg	ter	qua	qui	sex	sáb
31	1	2	3	4	5	6
7	8	9	10	11	12	13
14	15	16	17	18	19	20
21	22	23	24	25	26	27
28						

março de 2021						
dom	seg	ter	qua	qui	sex	sáb
	1	2	3	4	5	6
7	8	9	10	11	12	13
14	15	16	17	18	19	20
21	22	23	24	25	26	27
28	29	30	31			

abril de 2021						
dom	seg	ter	qua	qui	sex	sáb
				1	2	3
4	5	6	7	8	9	10
11	12	13	14	15	16	17
18	19	20	21	22	23	24
25	26	27	28	29	30	

maio de 2021						
dom	seg	ter	qua	qui	sex	sáb
						1
2	3	4	5	6	7	8
9	10	11	12	13	14	15
16	17	18	19	20	21	22
23	24	25	26	27	28	29
30	31					

junho de 2021						
dom	seg	ter	qua	qui	sex	sáb
		1	2	3	4	5
6	7	8	9	10	11	12
13	14	15	16	17	18	19
20	21	22	23	24	25	26
27	28	29	30			

julho de 2021						
dom	seg	ter	qua	qui	sex	sáb
				1	2	3
4	5	6				

Hoje: 06/07/2021

Date:

Session Hour:

Session Type:

Affected Side:

Trials:

Walking:


Flexibility:

Knee Outcome Survey

Pain	- The symptom prevents me from all daily activity
Stiffness	- The symptom prevents me from all daily activity
Swelling	- The symptom prevents me from all daily activity
Giving way, buckling, or shifting of the knee	- The symptom prevents me from all daily activity
Weakness	- The symptom prevents me from all daily activity
Limping	- The symptom prevents me from all daily activity
Walk	- I am unable to do the activity
Go up stairs	- I am unable to do the activity
Go down stairs	- I am unable to do the activity
Stand	- I am unable to do the activity
Kneel on front of your knee	- I am unable to do the activity
Squat	- I am unable to do the activity
Sit with your knee bent	- I am unable to do the activity
Rise from a chair	- I am unable to do the activity

OBSERVATIONS

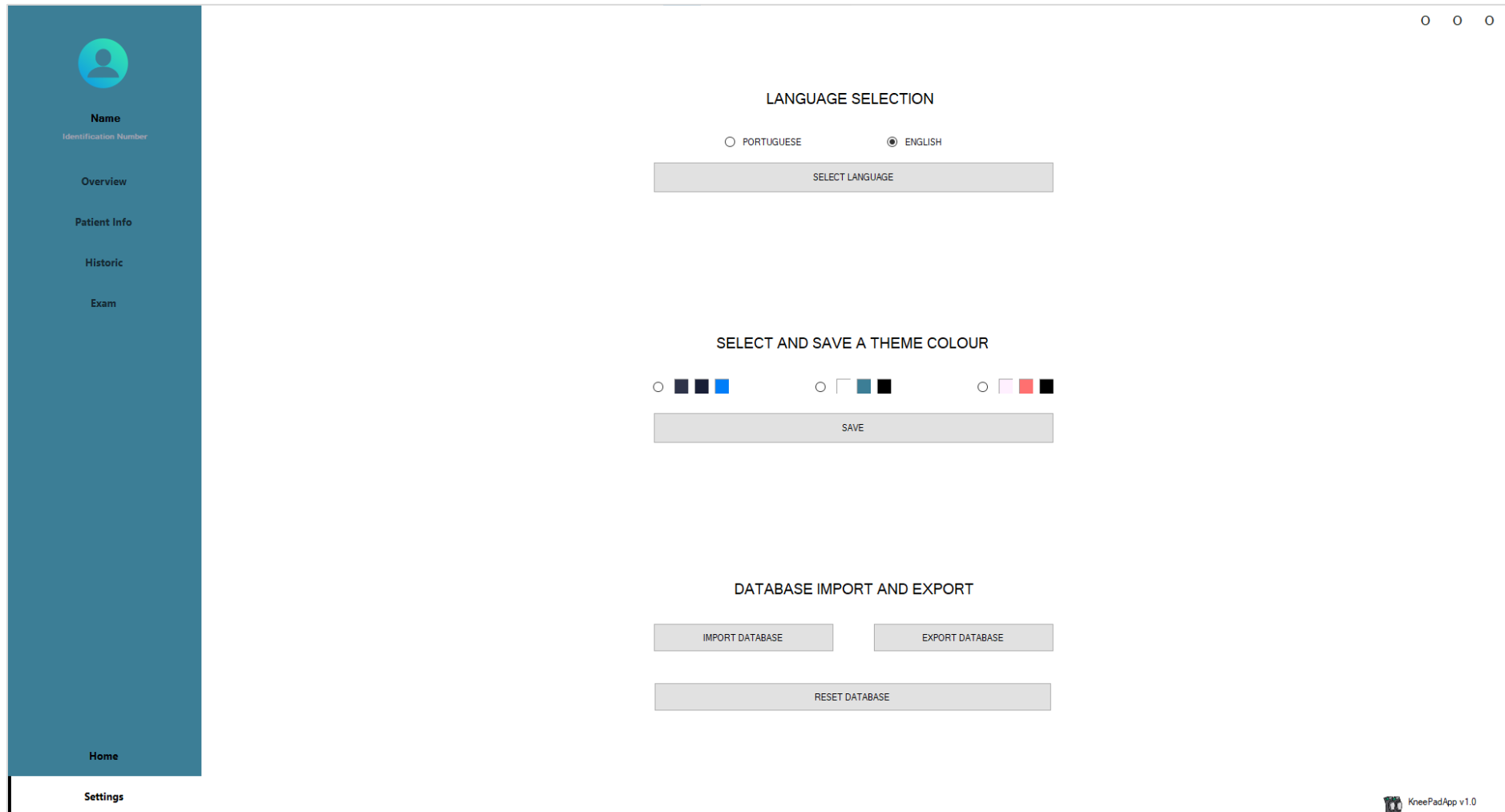
andar torto



Historic Page > It is presented the exams informations and observations by date.

The screenshot displays the 'Exam' page of the KneepadApp v1.0. On the left is a dark blue sidebar with a user profile for Antonio Madaleno and navigation options: Overview, Patient Info, Historic, Exam (selected), Home, and Settings. The main content area is divided into several sections: 1. TRIAL: A panel with radio buttons for 'Flexibility Test' and 'Walk Test', an 'ADD TEST' button, and a box labeled 'EXEMPLE TEST'. Below this is a 'START' button. 2. DISCONNECTED: A status indicator with a dropdown menu. 3. LEFT LEG and RIGHT LEG: Two columns of input fields for 'ANGLE [°]' and 'TIME [ms]', with 'STOP' buttons below each. 4. OBSERVATIONS: A large empty text area for recording observations. 5. REGISTRATION: Fields for 'REGIST DATA: 06/07/2021' and 'REGIST HOUR: 23:16', an 'ADD KNEE OUTCOME SURVEY' button, and dropdown menus for 'SESSION TYPE' and 'AFFECTED LEG'. 6. SAVE: A large button at the bottom right. 7. Host Name: 'DESKTOP-I11PCA9' is displayed above the save button. The bottom right corner shows the app logo and version 'KneePadApp v1.0'.

Exam Page > Where to start and make observations of an exam.



Settings Page > Where to change the application layout and where to import and export the data tables.